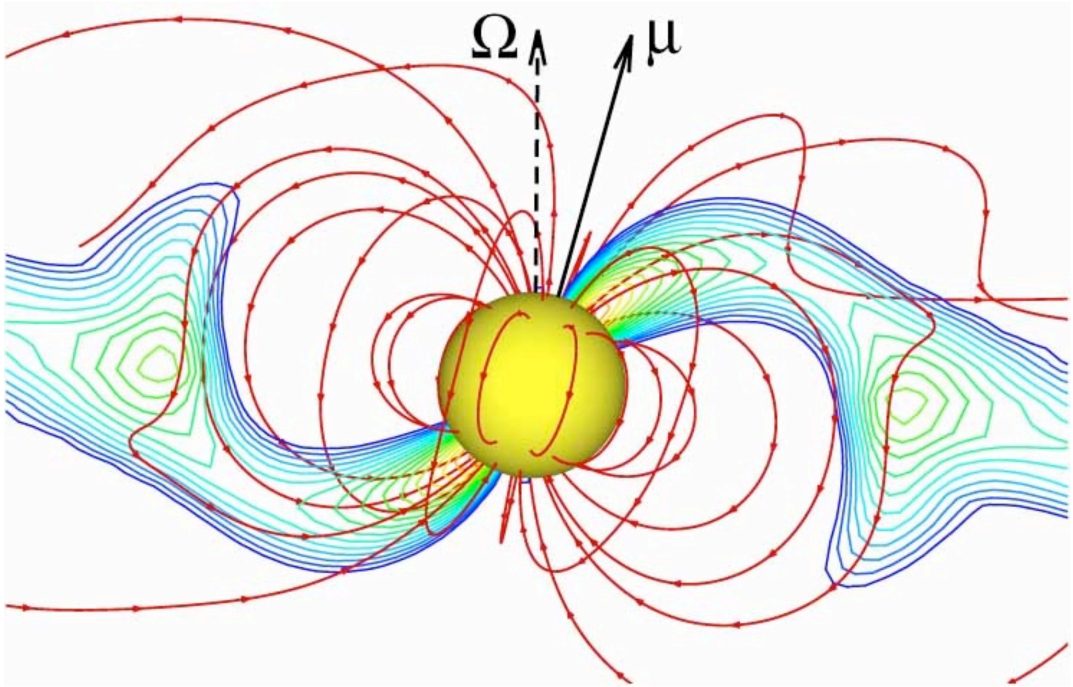

Polarized emission from accreting neutron stars as seen by the IXPE observatory

Sergey Tsygankov, + ...
(University of Turku)

UNIVERSITY OF TURKU

X-ray pulsars

High mass companions

Mass capture from wind/disk

High B-fields

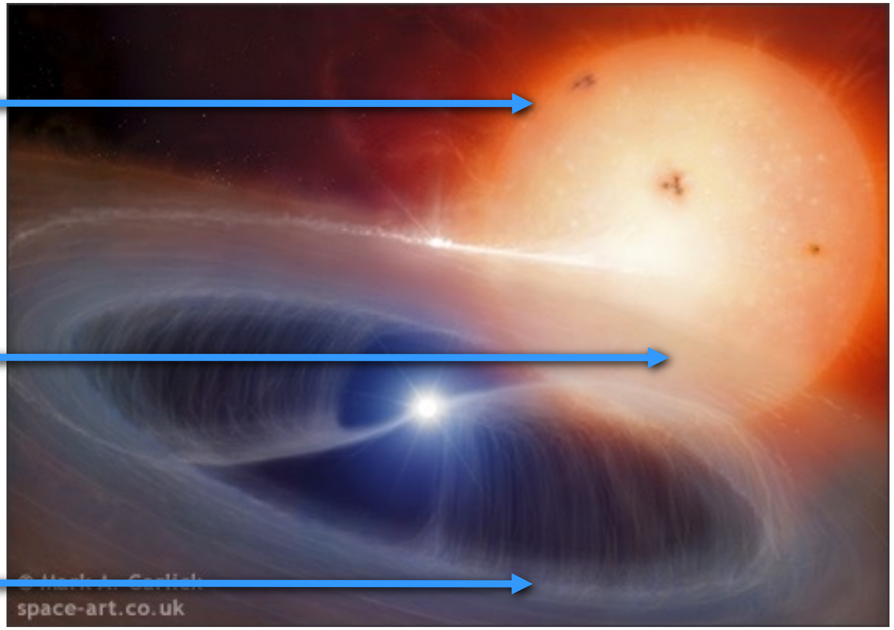

Disruption of disk by B-field

Matter channeled onto star

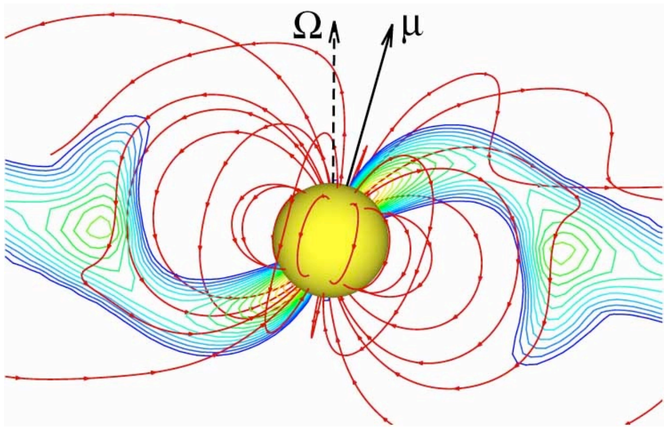

$P_{spin} \sim 1 - 10^3$ s

$B_{NS} \sim 10^{11\text{-}13}$ G

X-ray pulsars

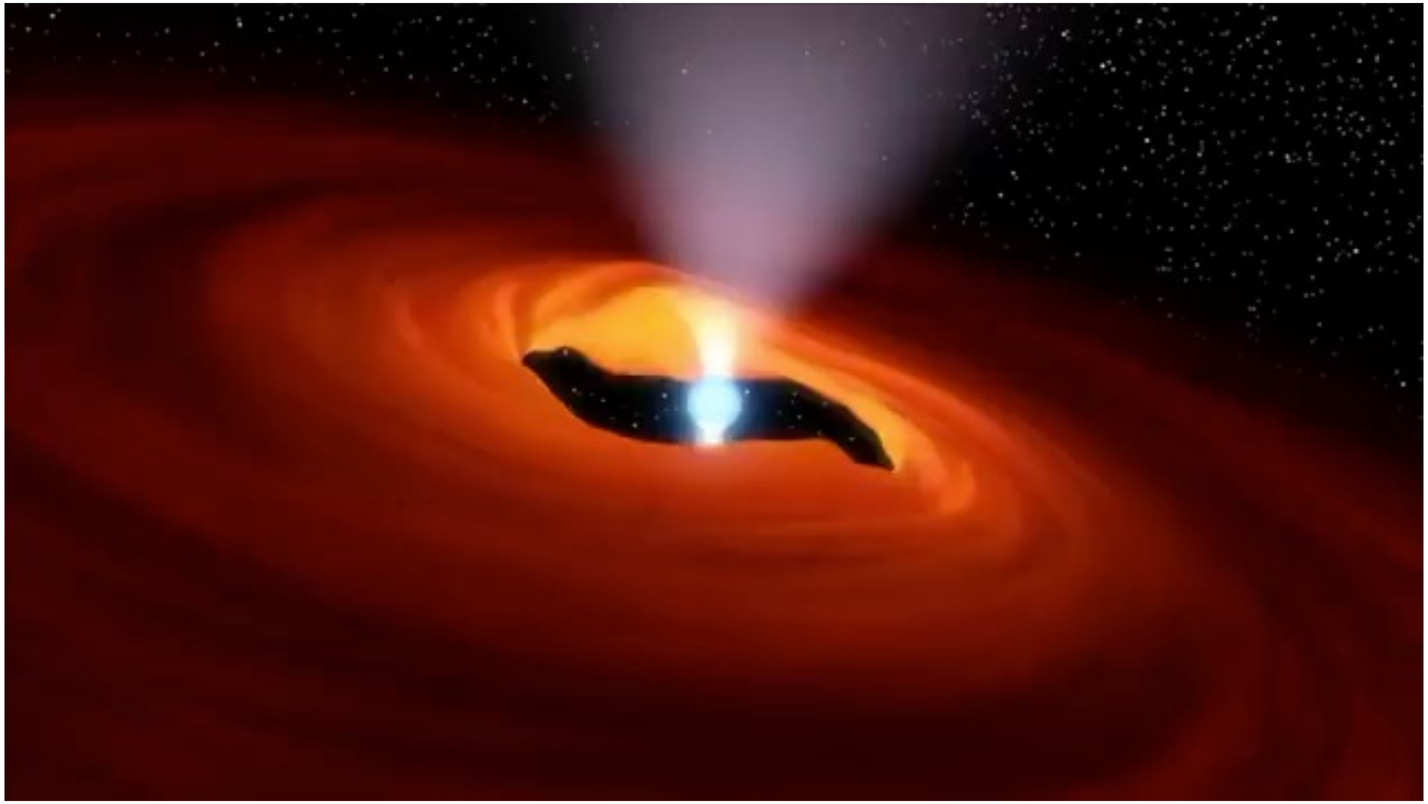

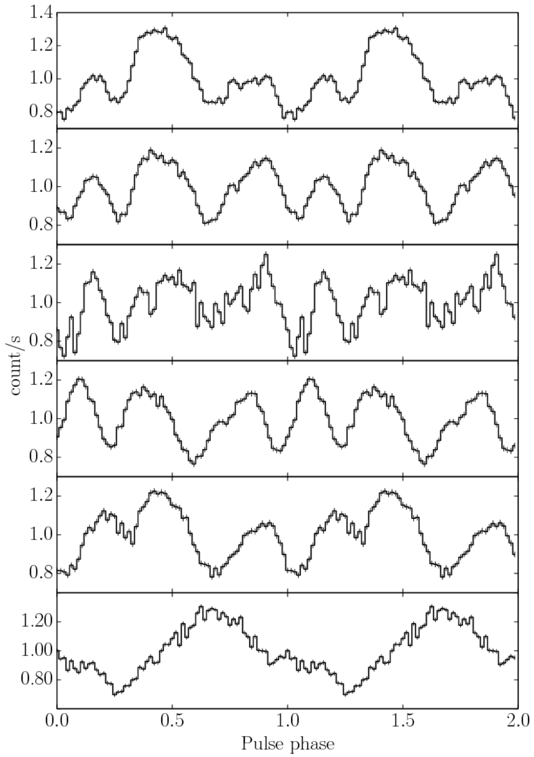

IXPE
Imaging
X-Ray
Polarimetry
Explorer

X-ray pulsars

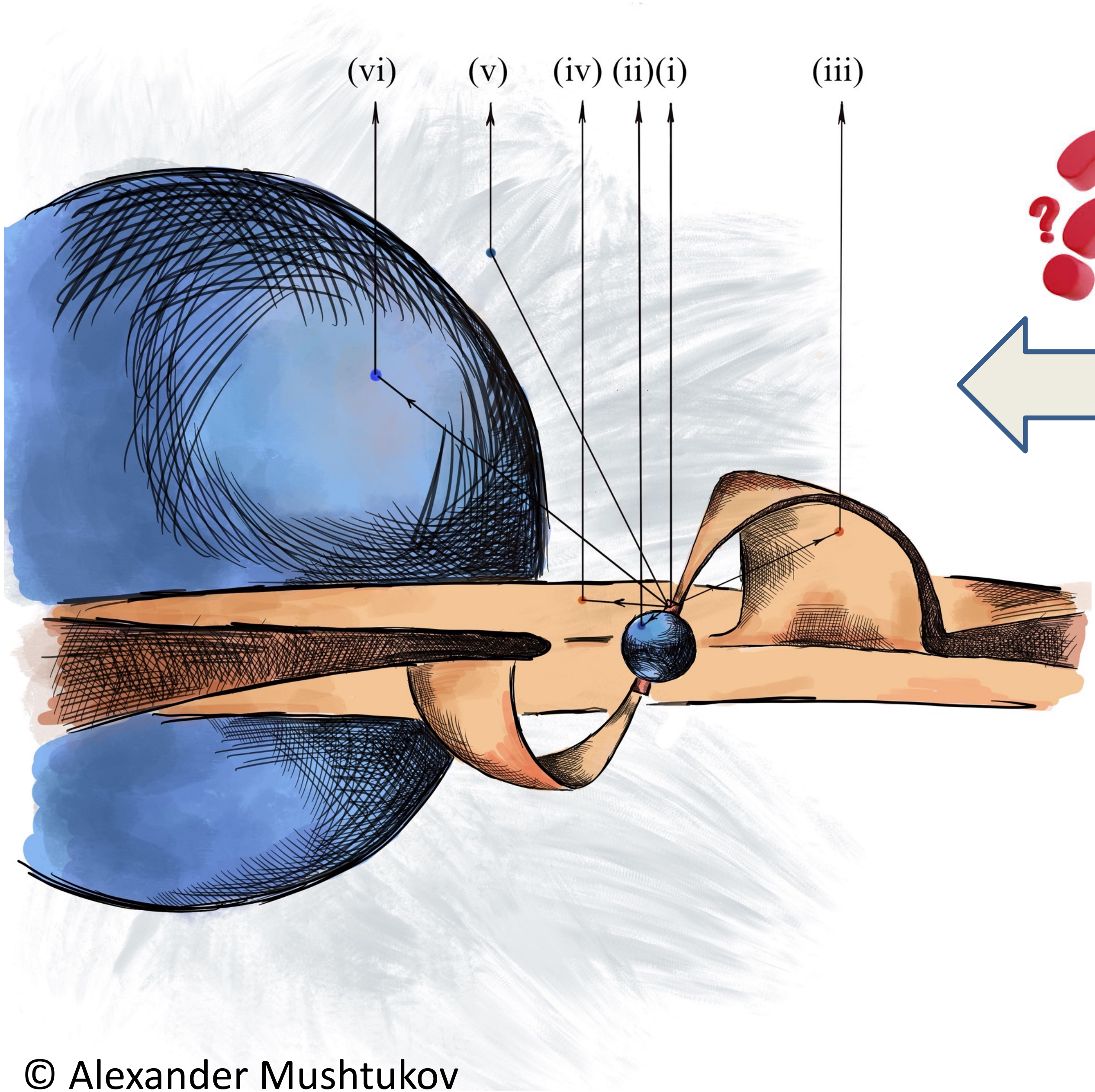

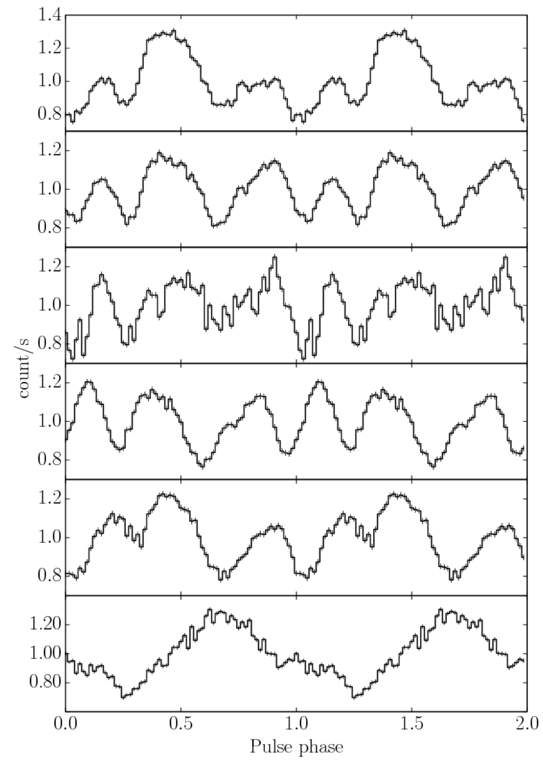

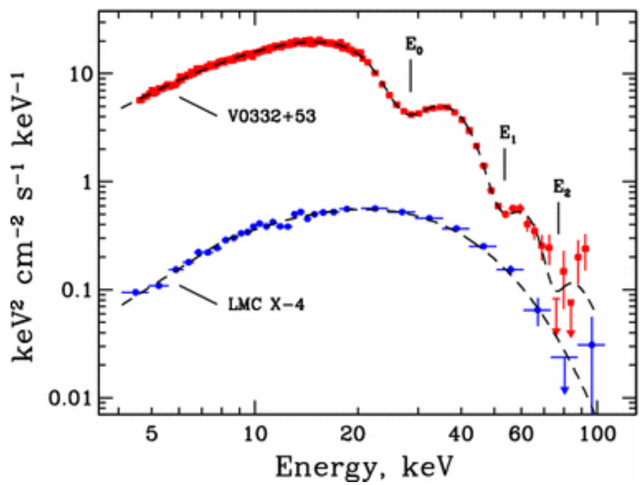

Geometry from polarimetry

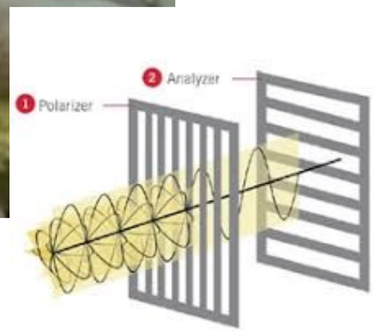

Geometry from polarimetry

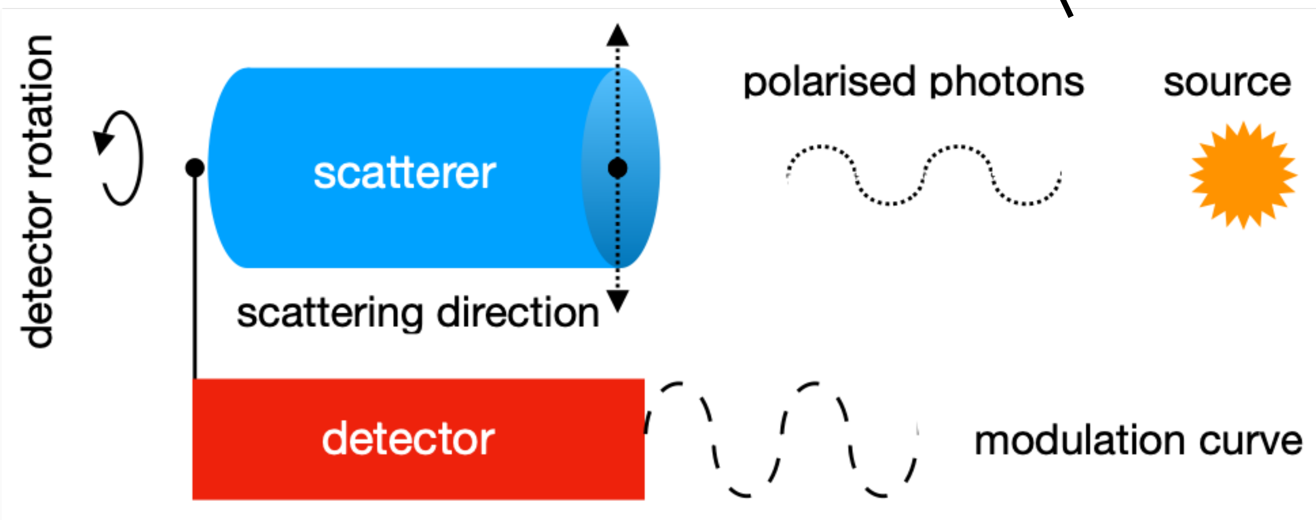

Polarimetry in X-rays

Linear polarization give us information on geometry: the degree depends on the level and kind of symmetry of the system, the angle indicates its orientation.

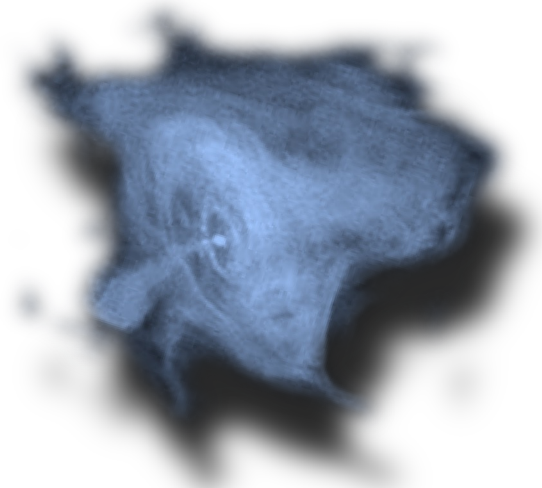

- First attempt to measure the X-ray polarization of the Crab Nebula back in 1969 with sounding rockets
  – PD<36% (Wolff et al. 1970)
- First X-ray nebula polarization measurement:
  PD=15.4%±5.2%, PA=156°±10° (5-20 keV)
  (Novick et al. 1972)
- New nebula polarization by OSO-8 with:
  PD=15.7%±1.5%, PA=161.1°±2.8° @2.6 keV
  PD=18.3%±4.2%, PA=155.5°±6.6° @5.2 keV
  (Weisskopf et al. 1976)
- After Pulsar subtraction (Weisskopf et al. 1978):
  PD=19.2%±1.0%, PA=156.4°±1.4° @2.6 keV
  PD=19.5%±2.8%, PA=152.6°±4.0° @5.2 keV

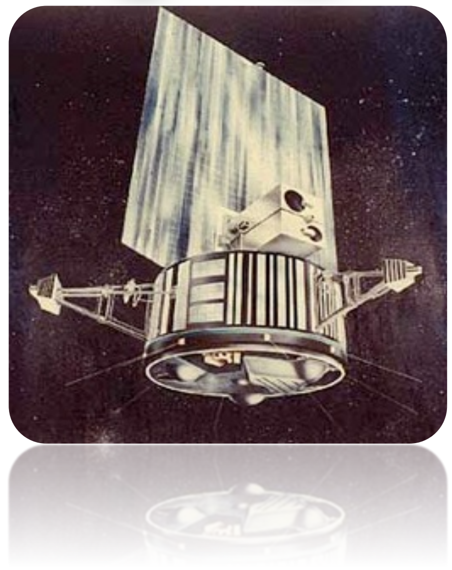

IXPE
Imaging
X-Ray
Polarimetry
Explorer

Map of polarized X-ray sources in 2021

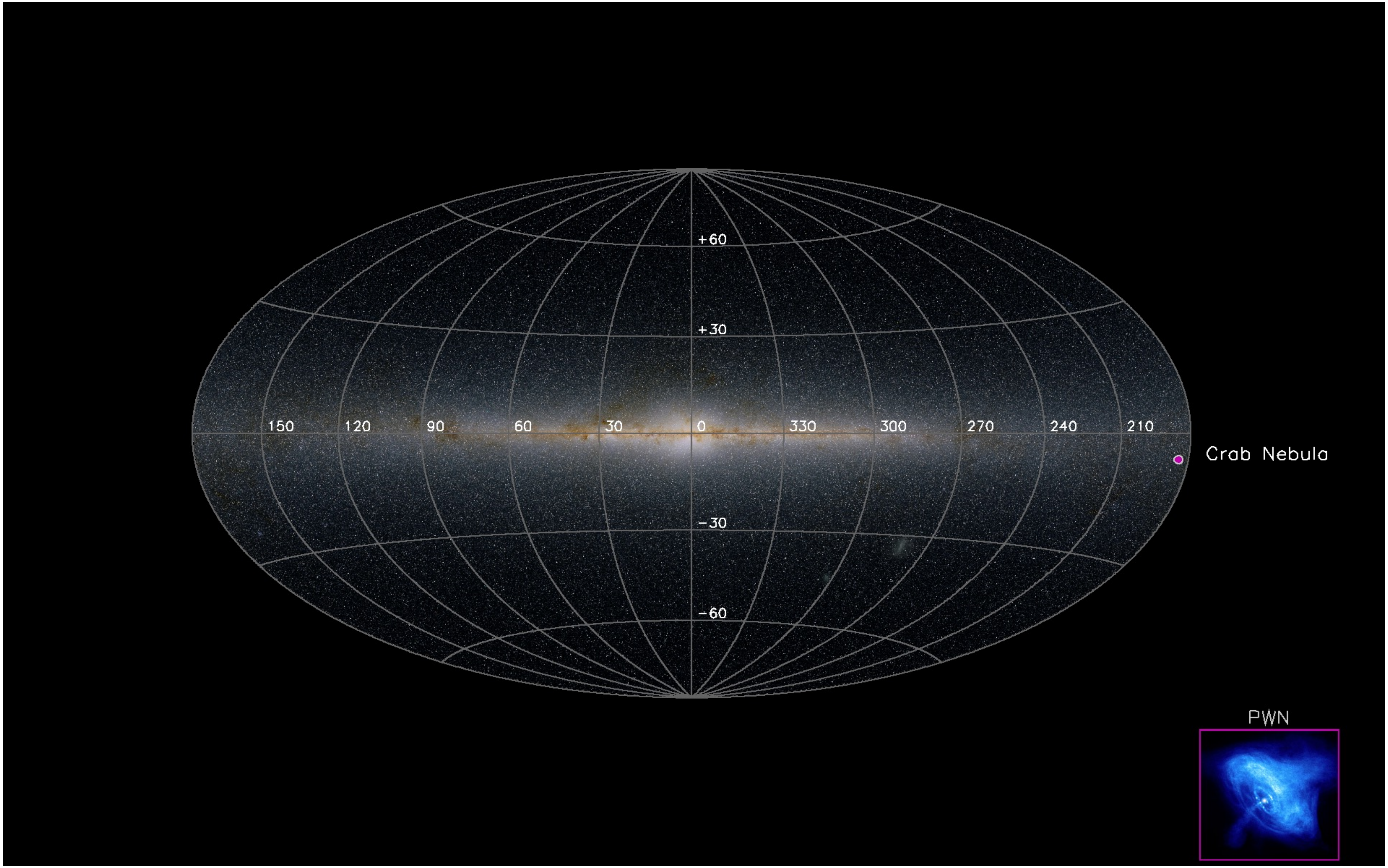

IXPE
Imaging
X-Ray
Polarimetry
Explorer

IXPE launched on 2021 Dec 9

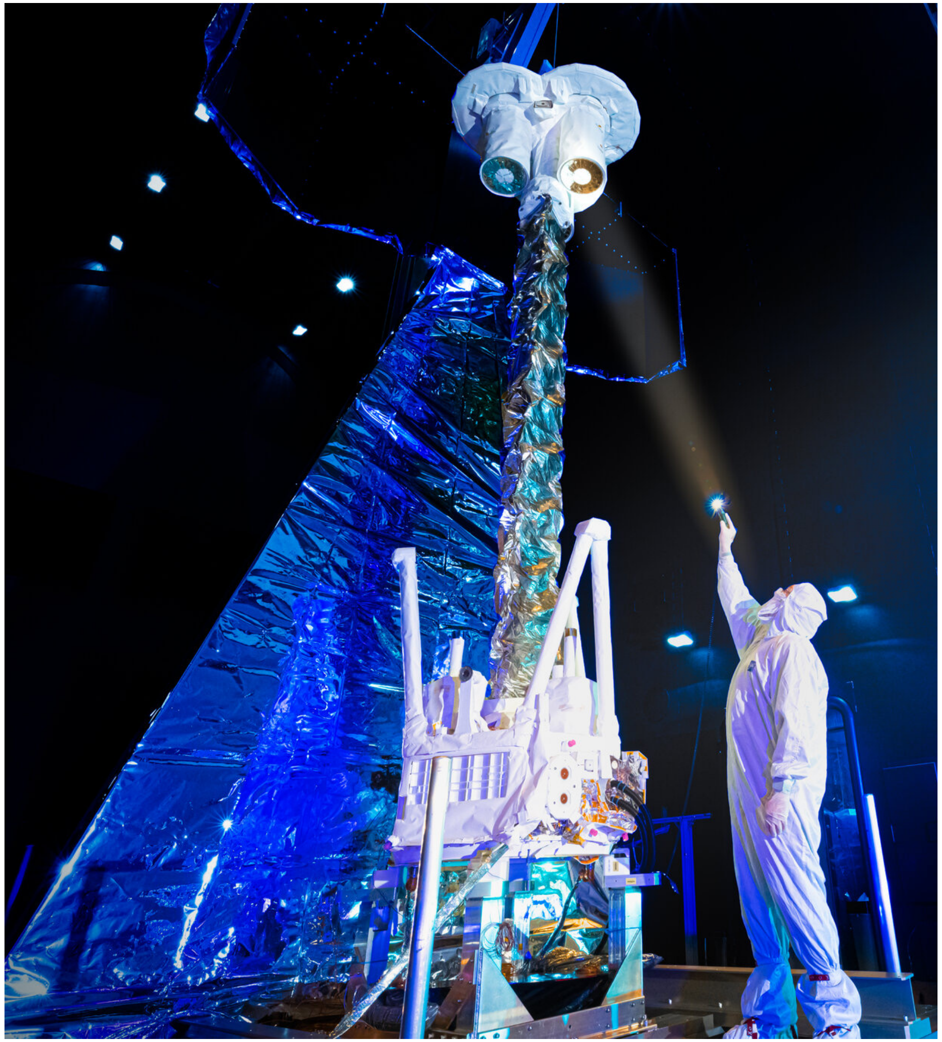

IXPE
Imaging
X-Ray
Polarimetry
Explorer

Imaging X-ray Polarimetry Explorer

Parameter	Value
Number of mirror modules	3
Number of shells per mirror module	24
Focal length	4 m
Total shell length	600 mm
Range of shell diameters	162–272 mm
Range of shell thicknesses	0.16–0.25 mm
Shell material	Electroformed nickel–cobalt alloy
Effective area per mirror module	166 cm^2 (@ 2.3 keV); > 175 cm^2 (3–6 keV)
Angular resolution (HPD)	≤ 27 arcsec
Field of view (detector limited)	12.9 arcmin square

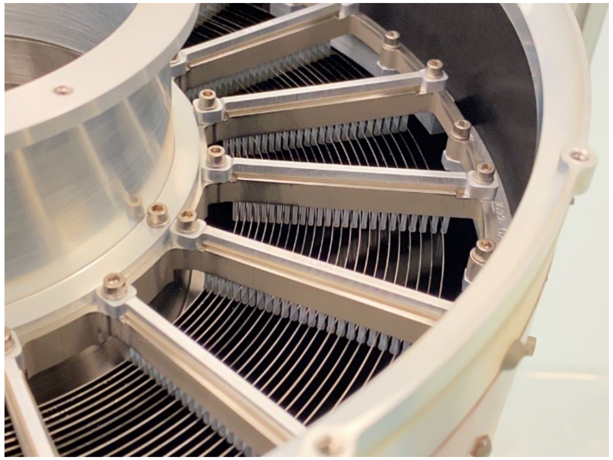

MMA, showing 24 shells

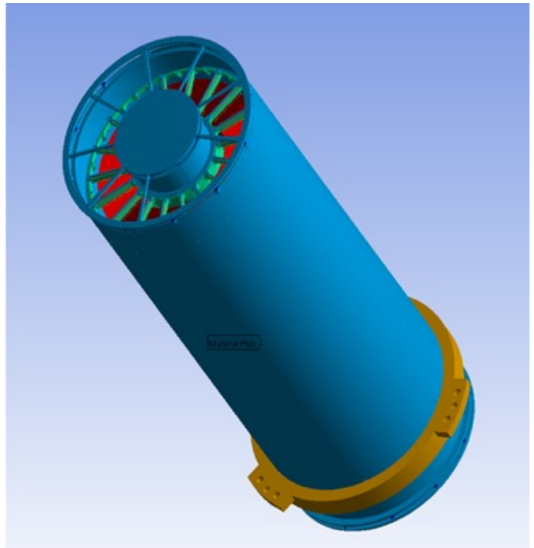

Three IXPE Mirror Module Assemblies

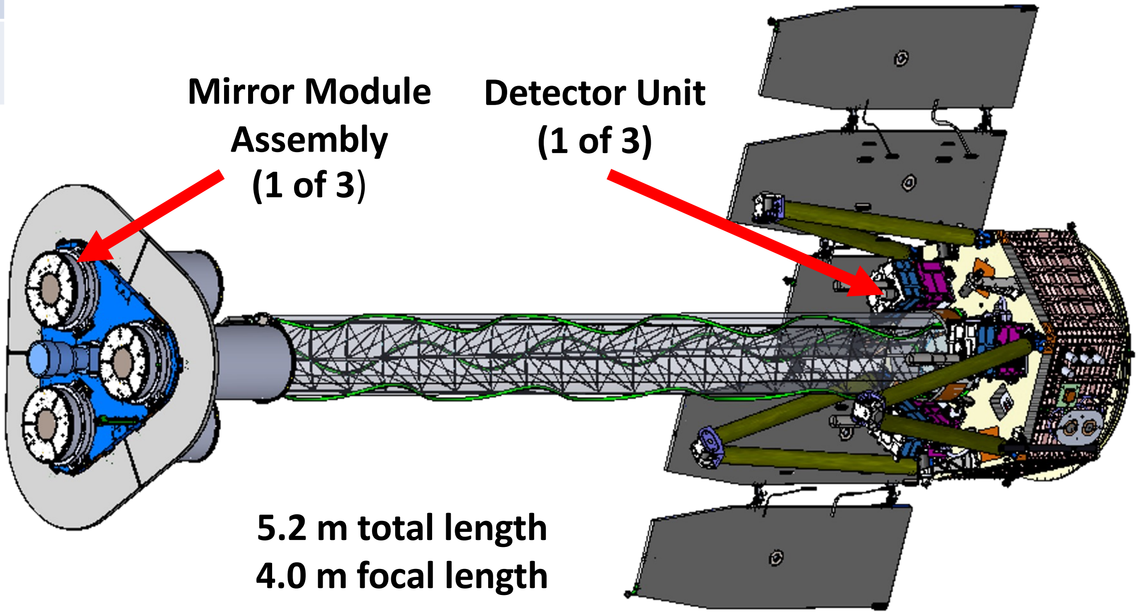

Detection Principle

- **The detection principle is based upon the photoelectric effect**

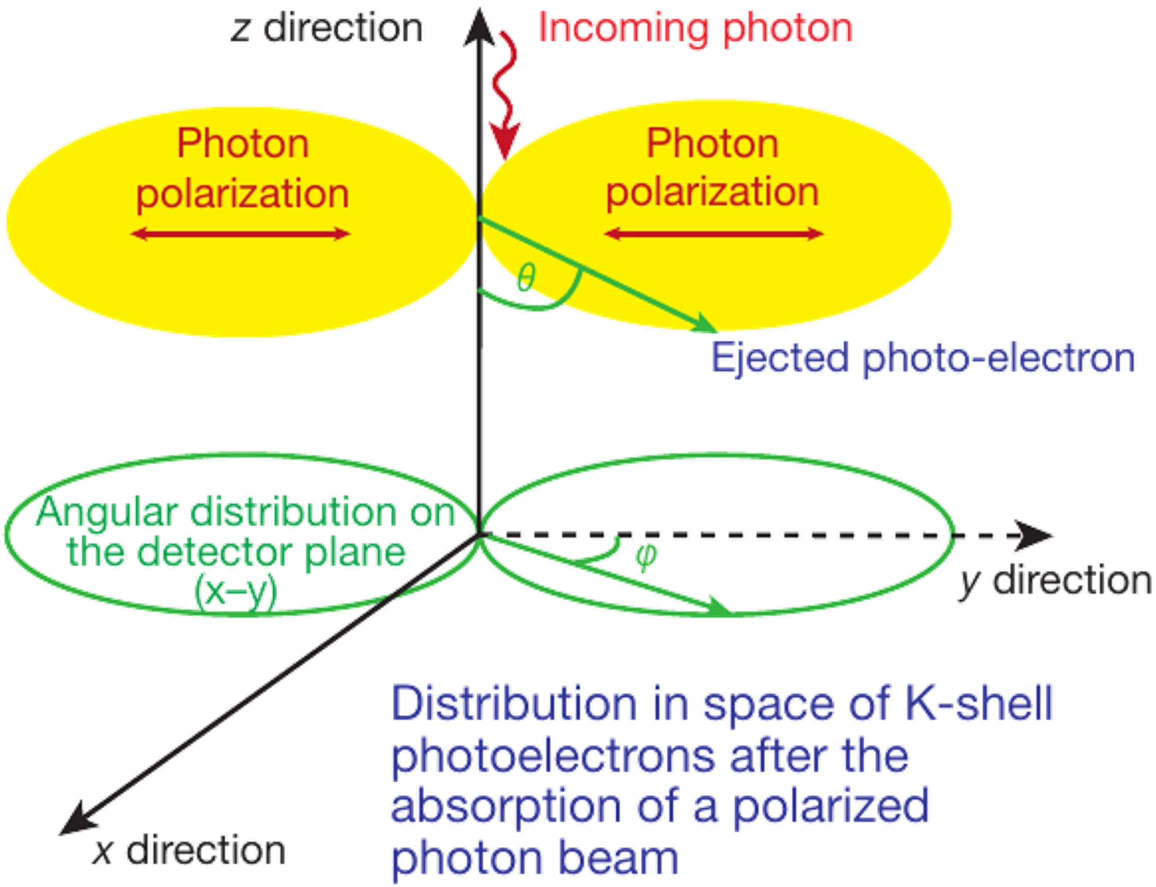

$$\frac{d\sigma}{d\Omega} = r_0^2 Z^5 \alpha_0^4 \left(\frac{1}{\beta}\right)^{7/2} 4\sqrt{2}\sin^2\theta\cos^2\varphi \;, \quad \text{where} \quad \beta \equiv \frac{E}{mc^2} = \frac{h\nu}{mc^2}$$

Gas Pixel Detector

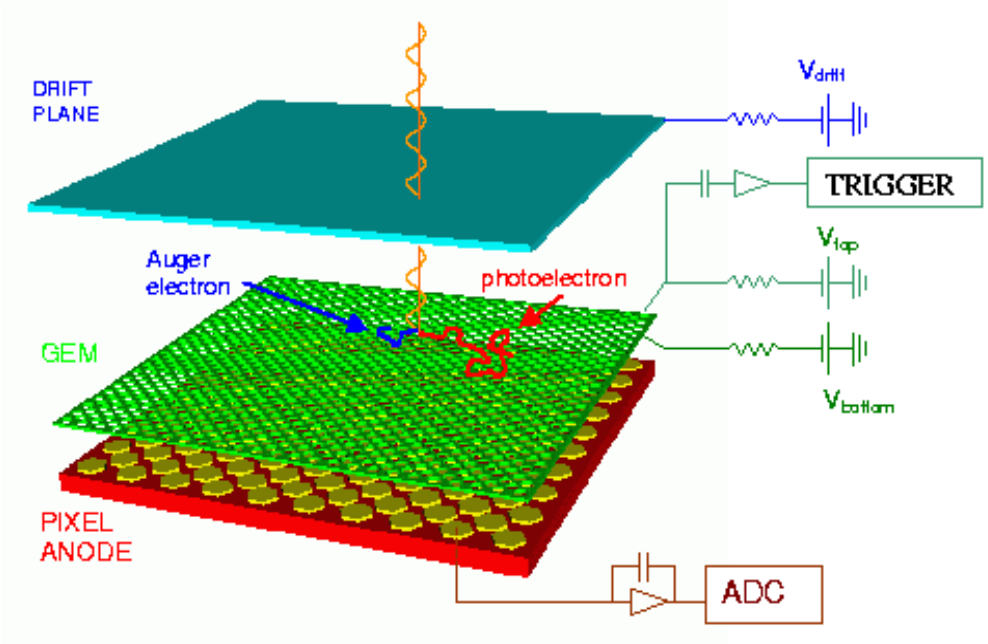

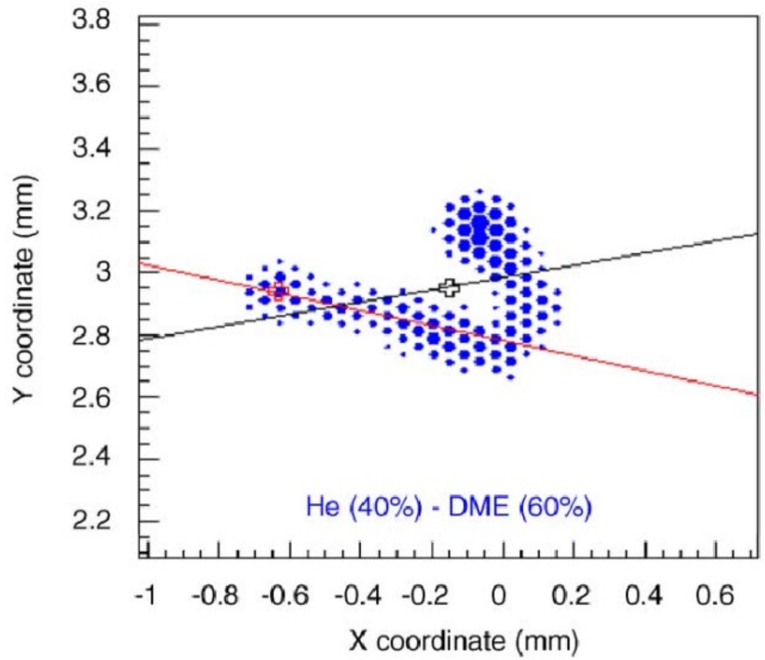

- Include a Filter & Calibration wheel with
  - Filters for specific observations (very bright sources, background)
  - Calibrations sources (polarized and unpolarized, gain)

POLARIZATION FROM MODULATION HISTOGRAM AND CALIBRATED MODULATION FACTOR

- **Polarization degree**
  - $\Pi = \text{Modulation}/\mu(E)$

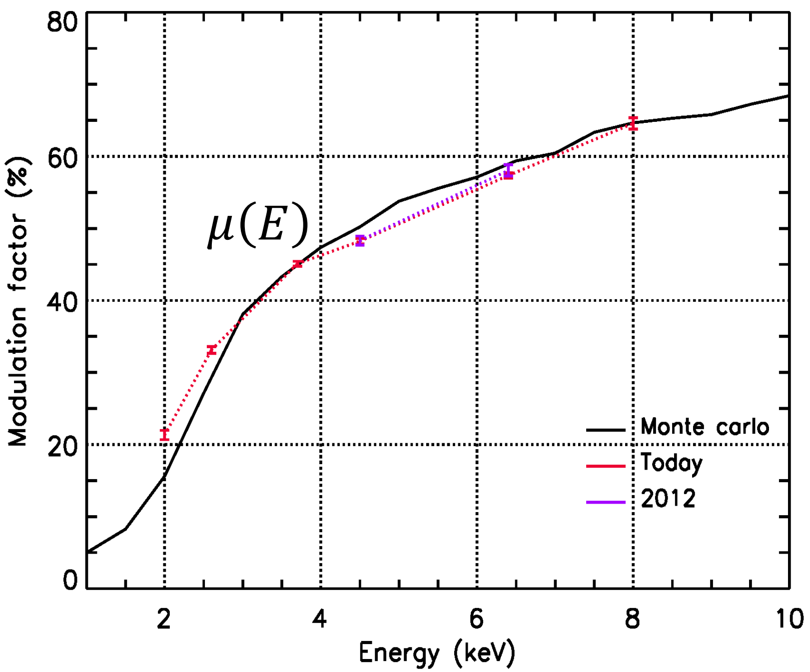

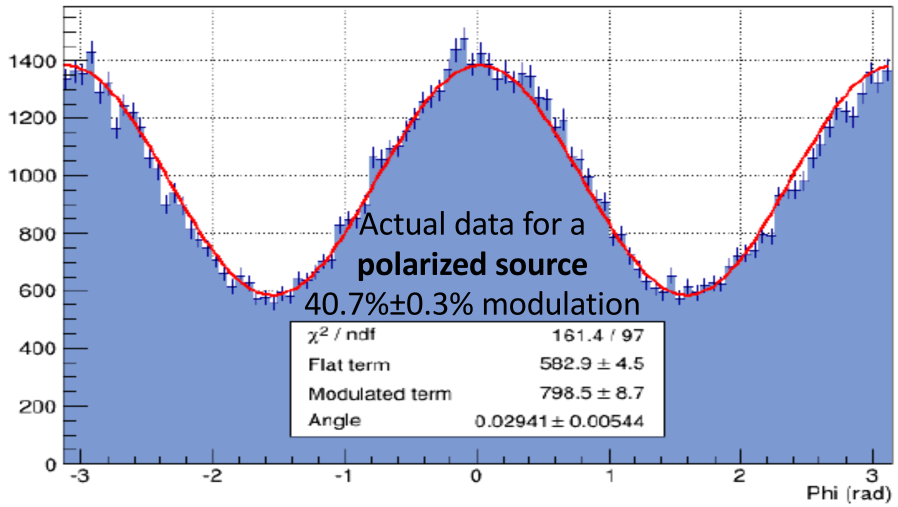

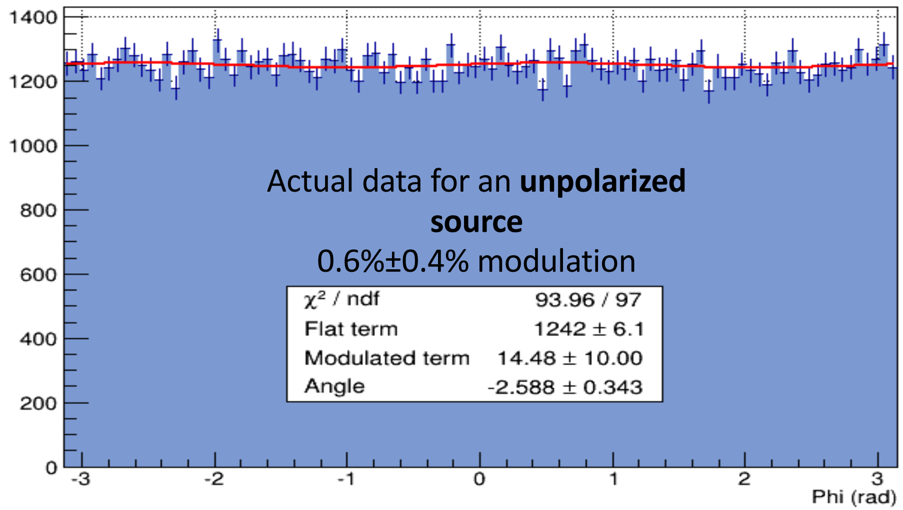

Marshall Space Flight Center

agenzia spaziale italiana

IXPE
Imaging
X-Ray
Polarimetry
Explorer

Sky map of X-ray polarized sources in 202(5?)

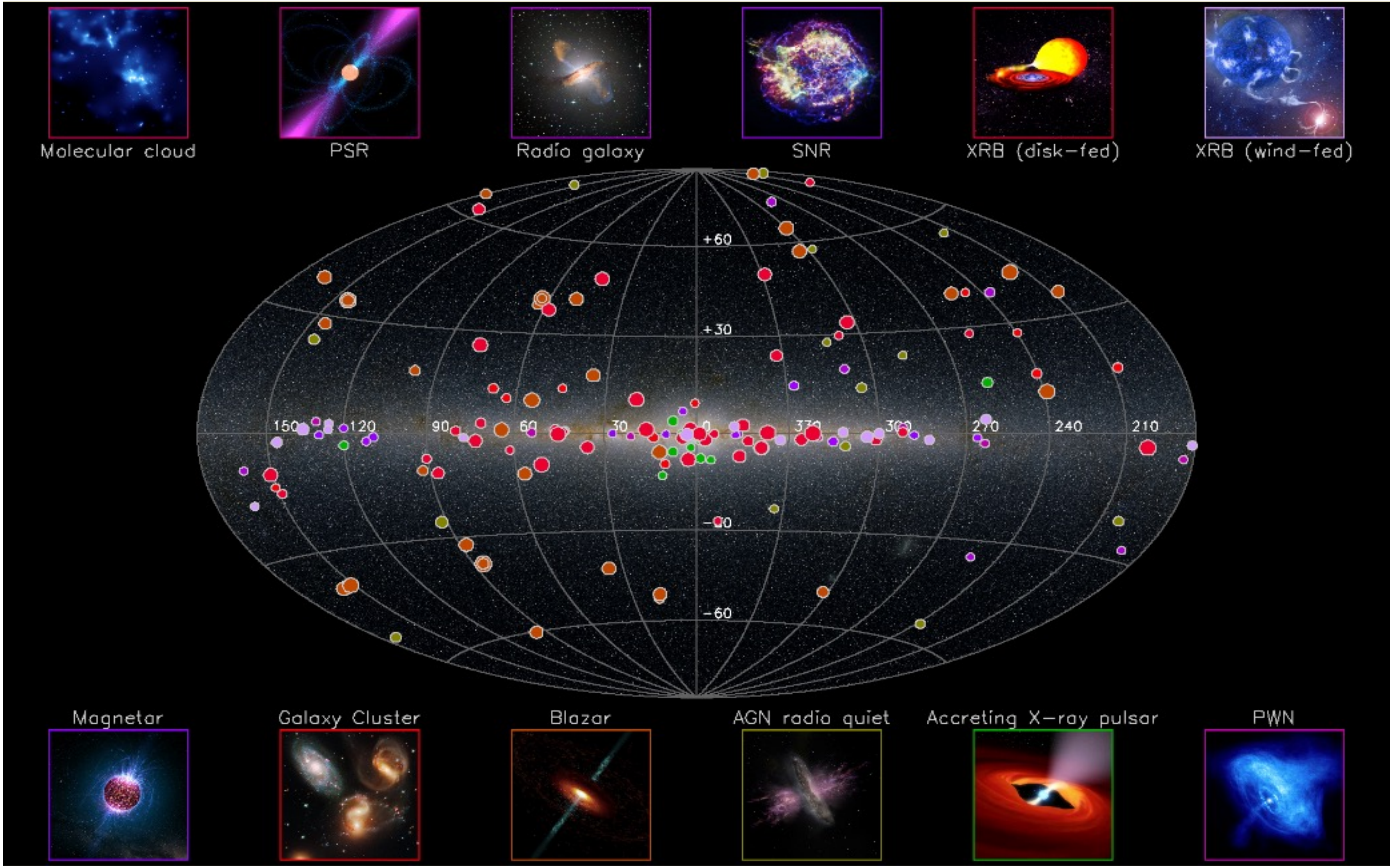

Polarization properties of X-ray pulsars

$e_{\parallel}$ – ordinary photons
$e_{\perp}$ – extraordinary photons

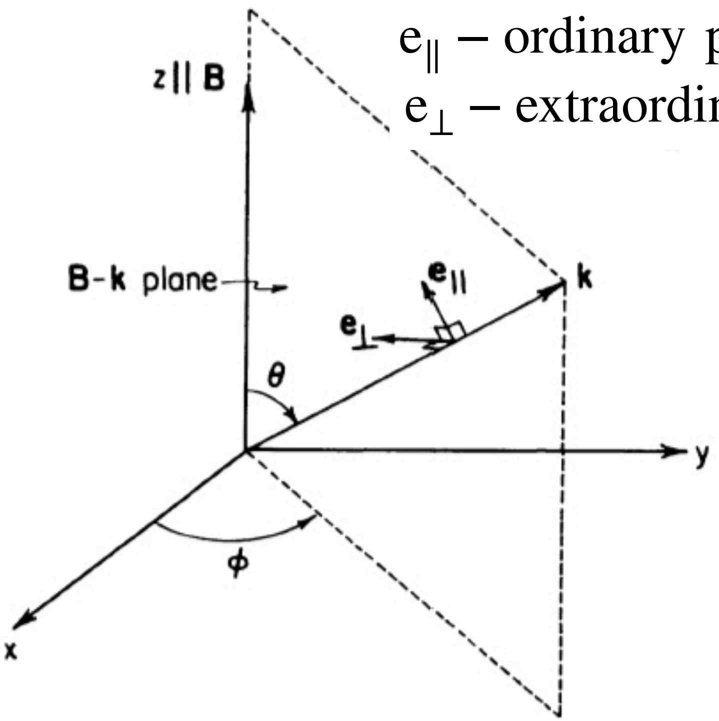

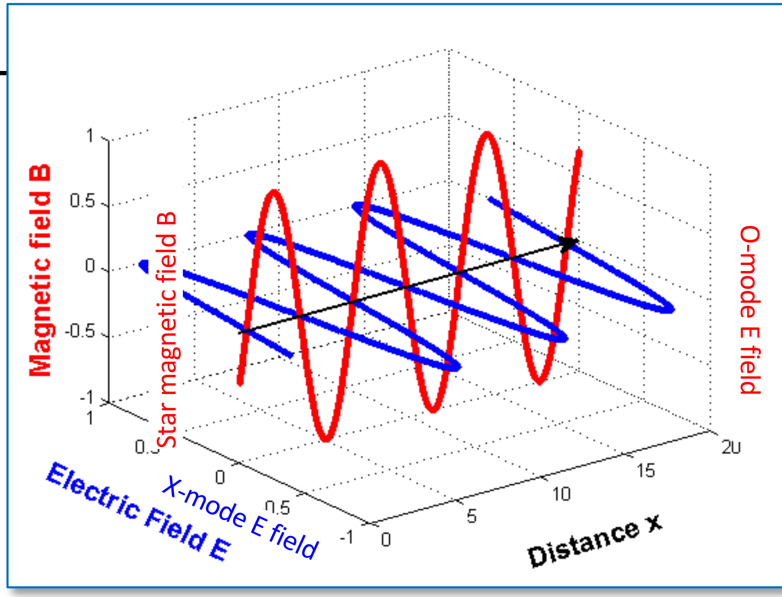

O-mode: the **E**-field oscillates in the **k-B** plane
X-mode: the **E**-field oscillates ⊥ to the **k-B** plane

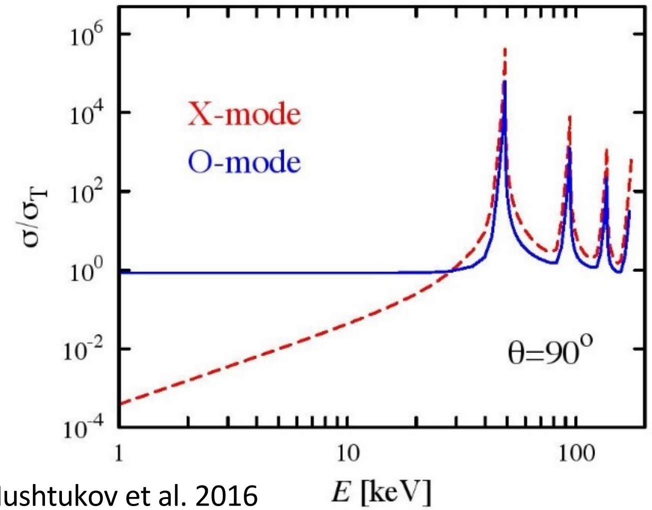

Mushtukov et al. 2016

The opacity of the X-mode is drastically reduced compared to that of the opacity of the O-mode. Consequently, the emergent radiation is dominated by the X-mode, which comes from the deeper and hotter layers of plasma, and so is strongly polarized in the direction of the X-mode.

Polarization properties of X-ray pulsars

Beam pattern of the emerging radiation is determined by the geometry of the emission region. Two main configurations of the emission regions can be distinguished depending on the local mass accretion rate.

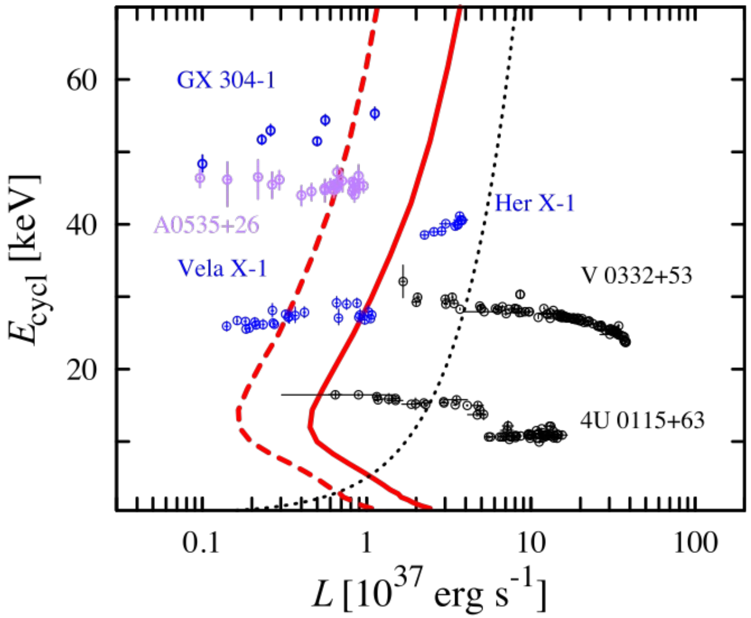

The critical luminosity L* separating these two regimes of accretion is a function of physical and geometrical parameters of the system and for typical XRP is estimated to be about 10^{37} erg/s (Basko & Sunyaev 1975; Becker et al. 2012; Mushtukov et al. 2015).

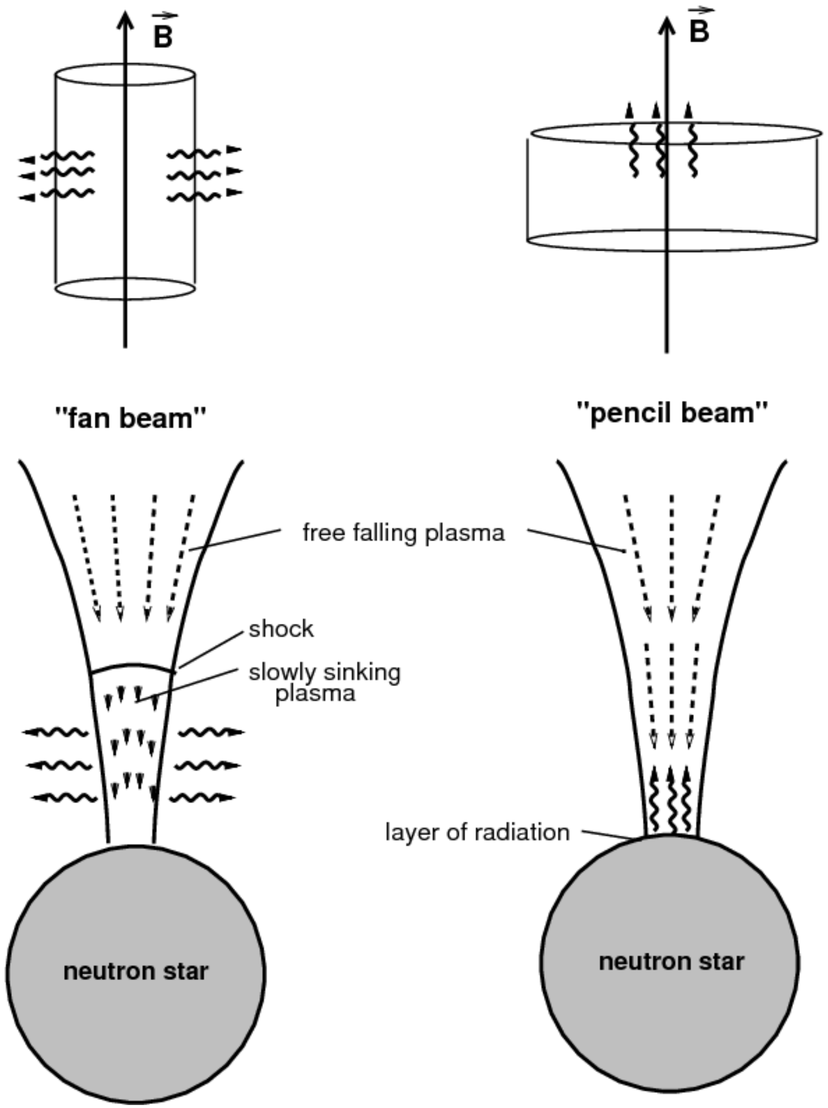

Polarization properties of X-ray pulsars

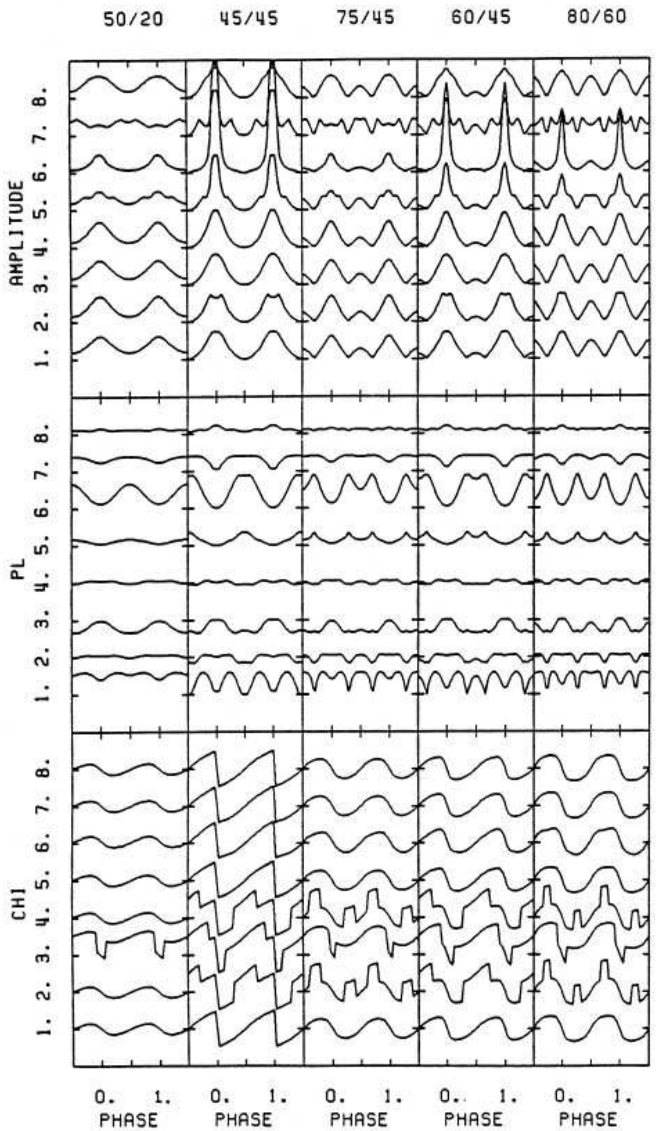

Pencil beam

Fan beam

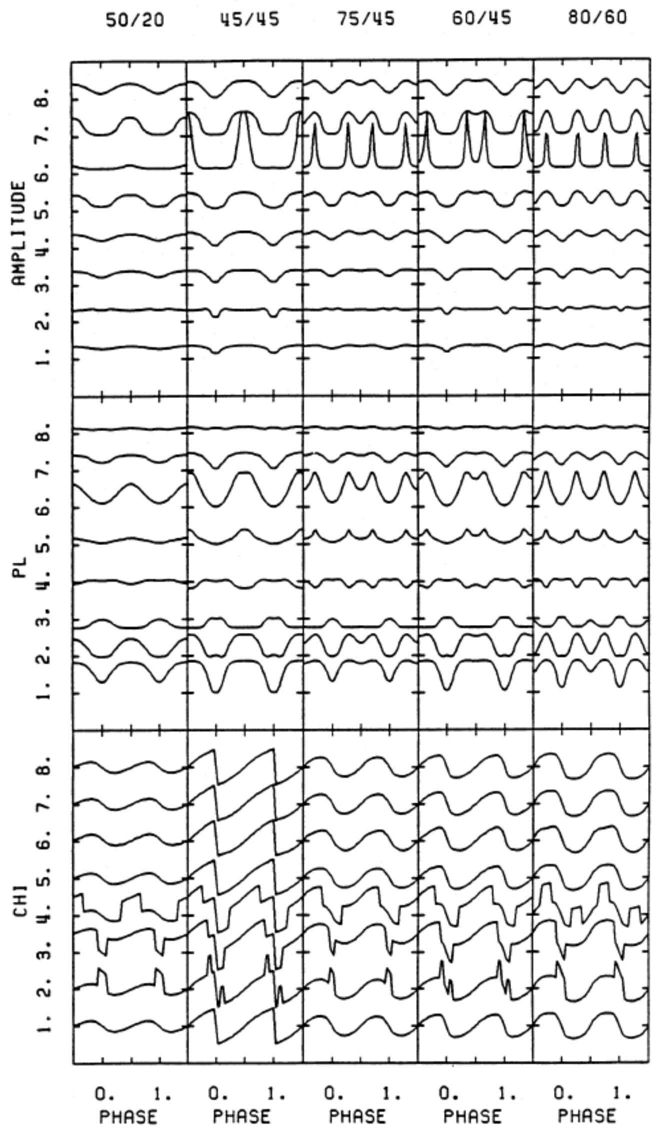

Meszaros et al. 1988

Polarization properties of X-ray pulsars

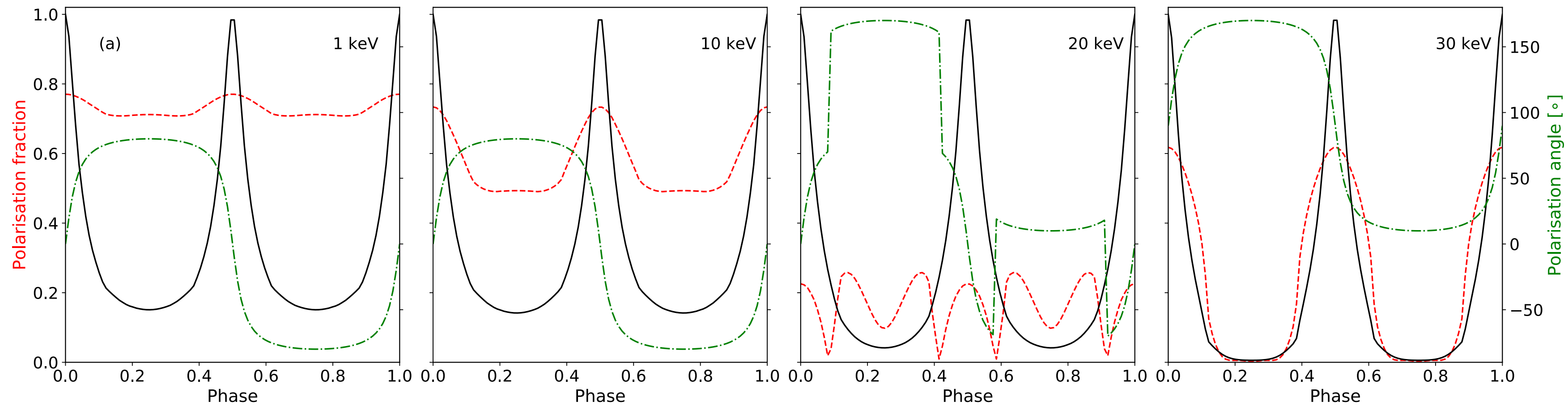

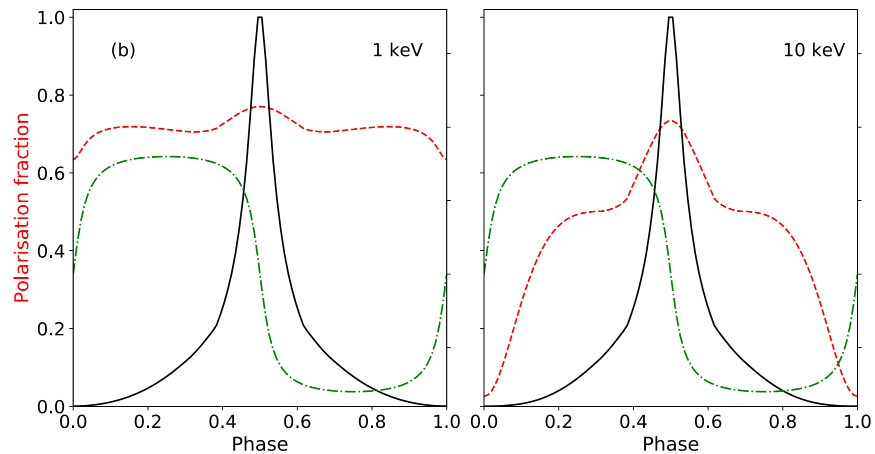

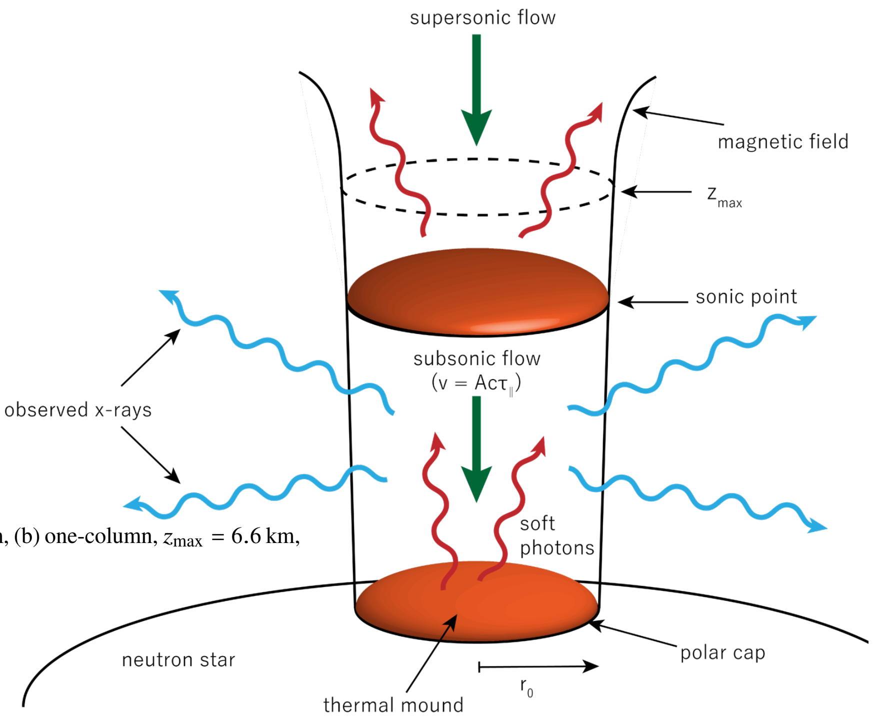

Figure 15. Polarisation parameters as a function of phase and energy for four different models: (a) two-column, $z_{\max} = 6.6$ km, (b) one-column, $z_{\max} = 6.6$ km,

Caiazzo & Heyl, 2021

X-ray pulsars observed by IXPE

Cen X-3 (ApJ Letters)
Her X-1 (Nature Astronomy)
4U 1626-67 (ApJ)
Vela X-1 (ApJ Letters)
GRO J1008-57 (A&A)
EXO 2030+375 (A&A)
X Per (MNRAS)
GX 301-2 (A&A)
More Her X-1 (Nature Astronomy)
LS V +44 17/RX J0440.9+4431 (A&A)
Swift J0243.6+6124 (submitted)
SMC X-1 (submitted)

X-ray pulsars observed by IXPE

Cen X-3 (ApJ Letters)
Her X-1 (Nature Astronomy)
4U 1626-67 (ApJ)
Vela X-1 (ApJ Letters)
GRO J1008-57 (A&A)
EXO 2030+375 (A&A)
X Per (MNRAS)
GX 301-2 (A&A)
More Her X-1 (Nature Astronomy)
LS V +44 17/RX J0440.9+4431 (A&A)
Swift J0243.6+6124 (submitted)
SMC X-1 (submitted)

Cen X-3

Persistent X-ray pulsar with almost circular orbit (e < 0.0016) around an O6–8 III supergiant V779 Cen of mass and radius of 20.5±0.7 $M_{\odot}$ and 12 $R_{\odot}$, respectively. Ash et al. (1999) determined the inclination of the system to be $70^{\circ}.2 \pm 2^{\circ}.7$.

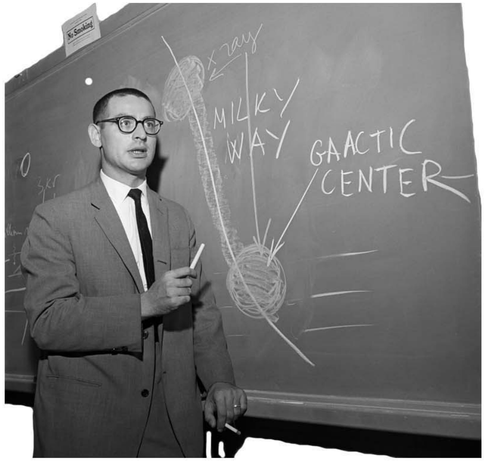

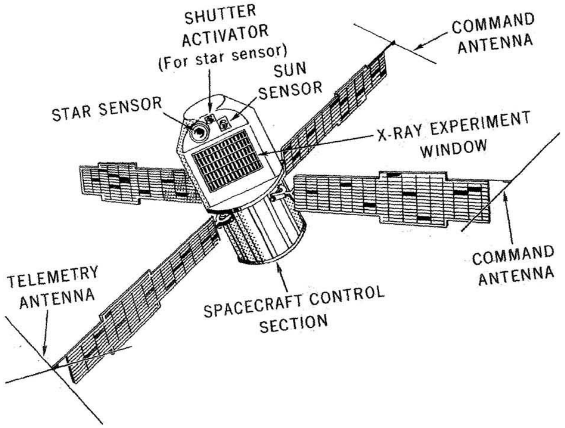

Spin period P_s=4.8 s
Orbital period P_{orb}=2.09 d
Distance d=$6.4^{+1.0}_{-1.4}$ kpc

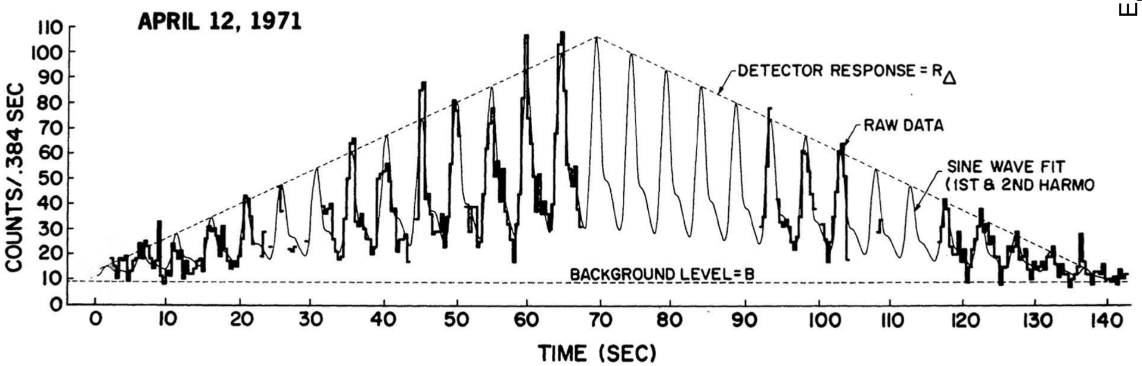

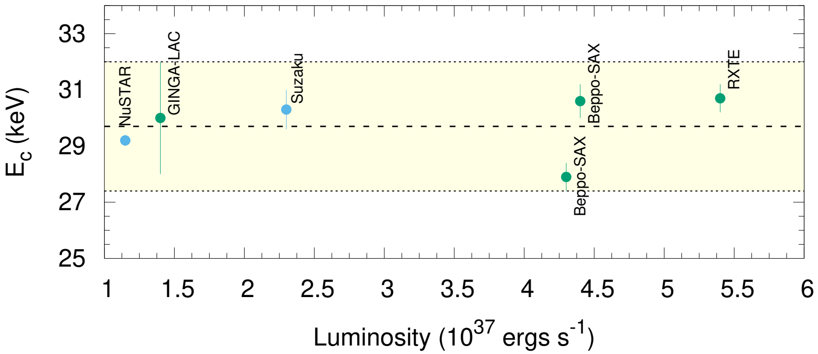

Tomar et al. 2021

IXPE observations

Long-term lightcurve

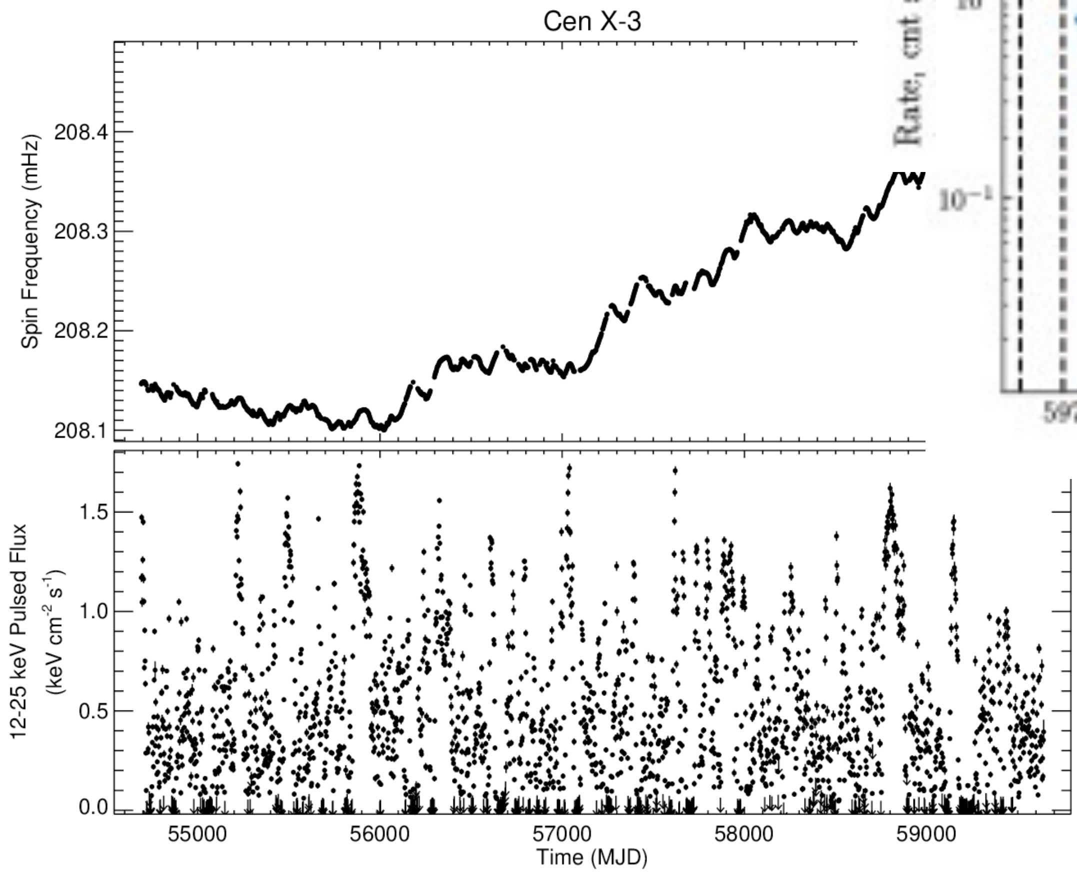

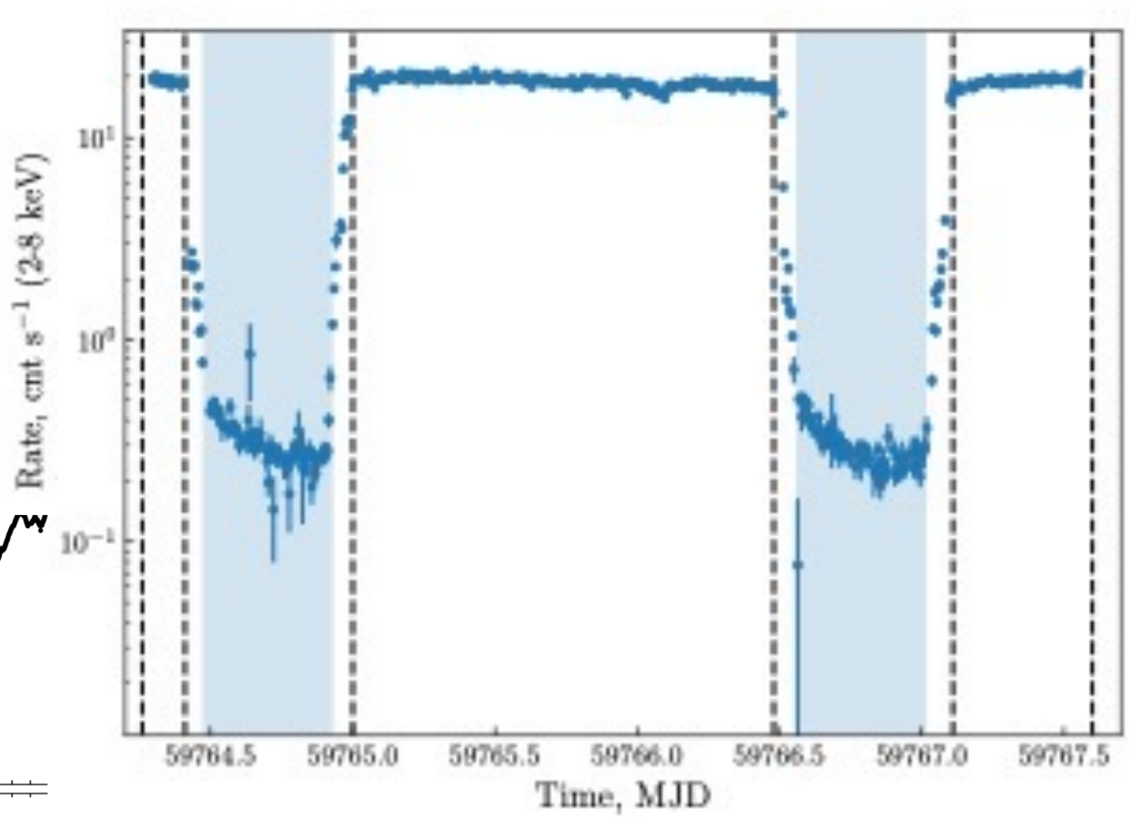

IXPE observations

Pulse phase-resolved polarimetry

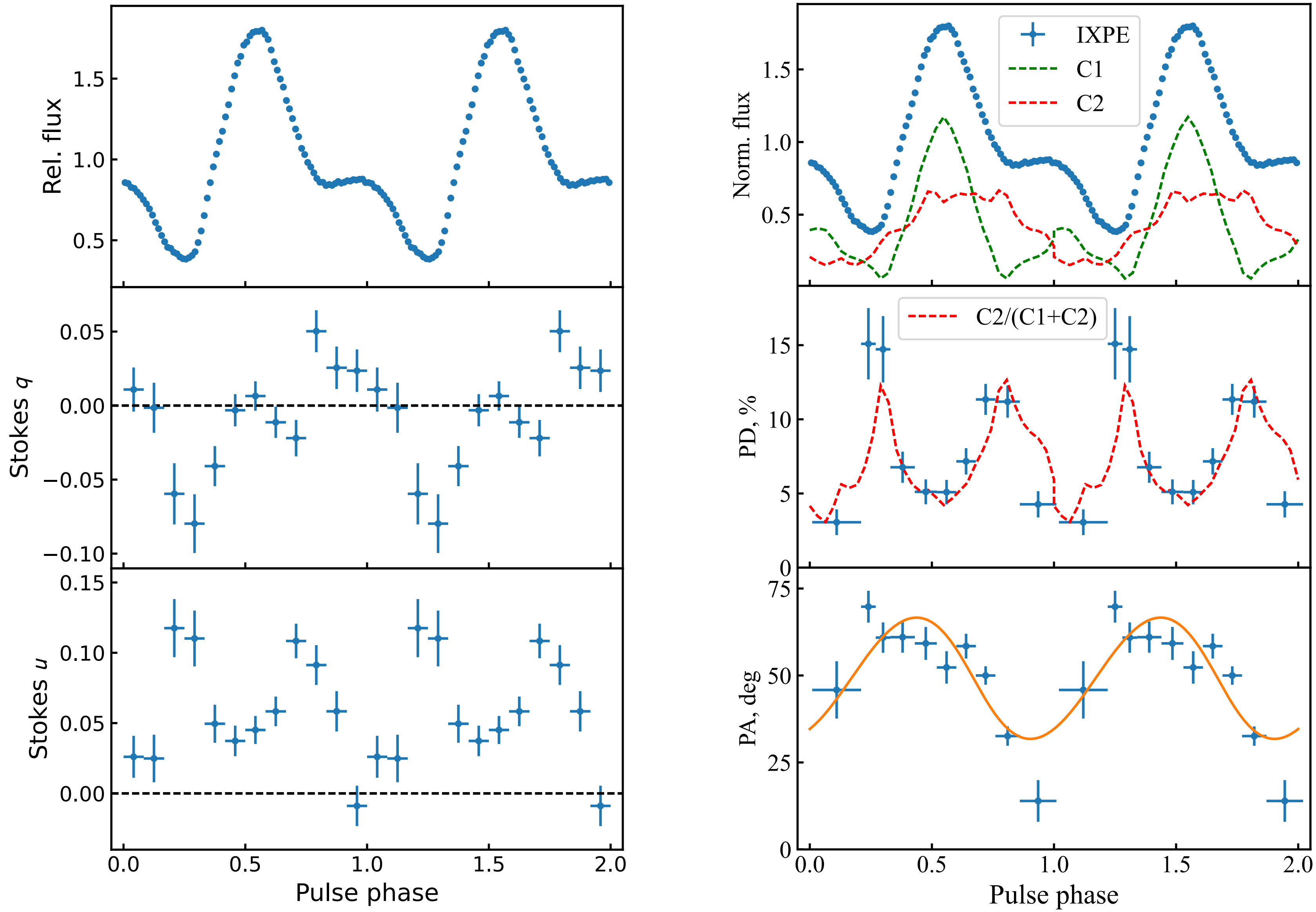

Tsygankov+, 2022, ApJL

Low polarization degree

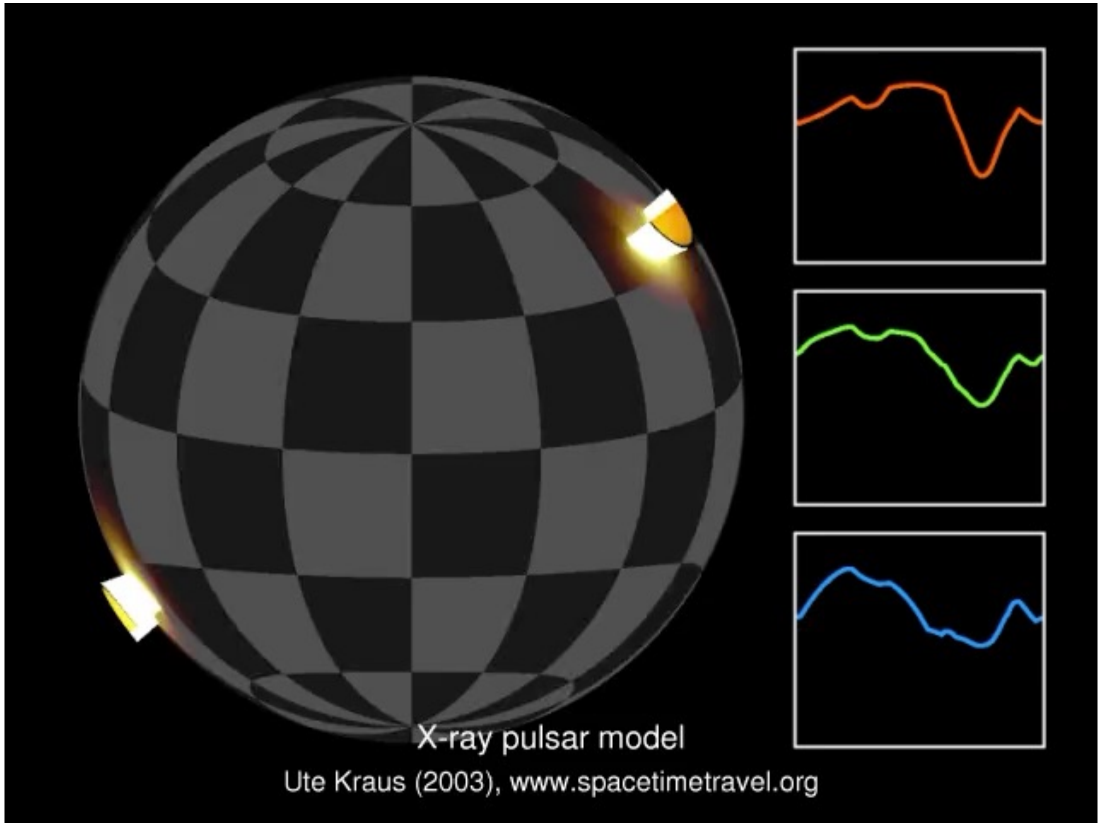

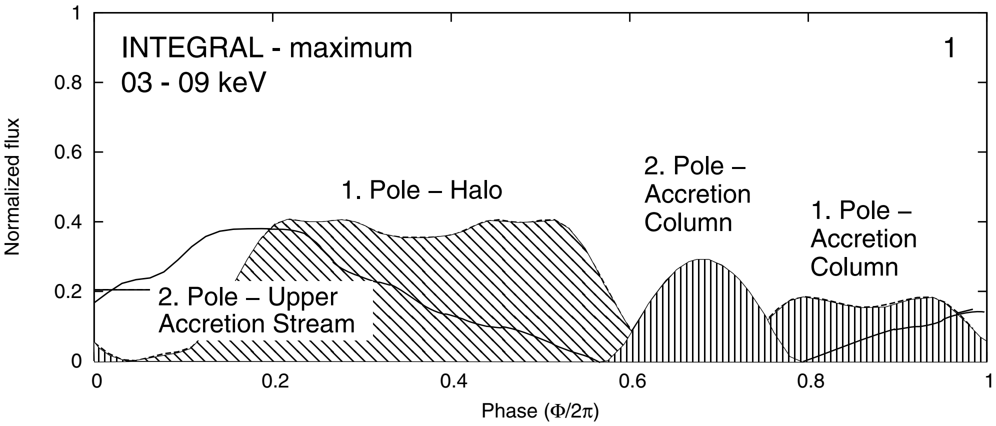

Kraus 96, 2003, Sasaki et al, 2012

IXPE
Imaging X-Ray Polarimetry Explorer

Geometry of the system

Rotating vector model

$$\tan(\mathrm{PA} - \chi_{\mathrm{p}}) = \frac{-\sin\theta\ \sin(\phi - \phi_0)}{\sin i_{\mathrm{p}}\ \cos\theta - \cos i_{\mathrm{p}}\ \sin\theta\ \cos(\phi - \phi_0)}$$

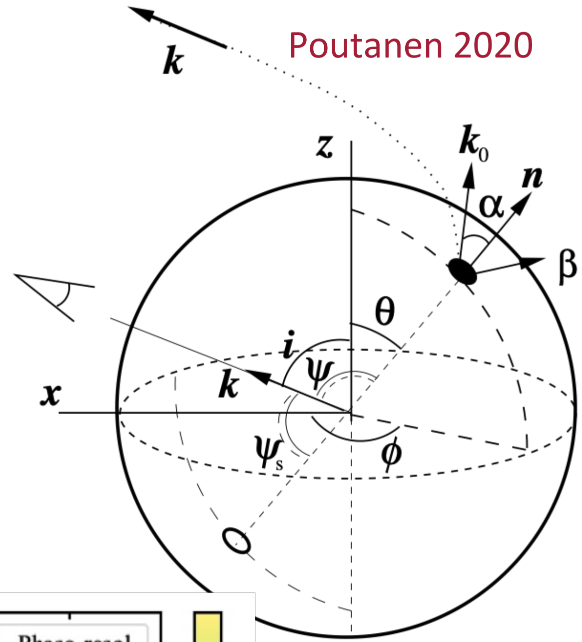

Poutanen 2020

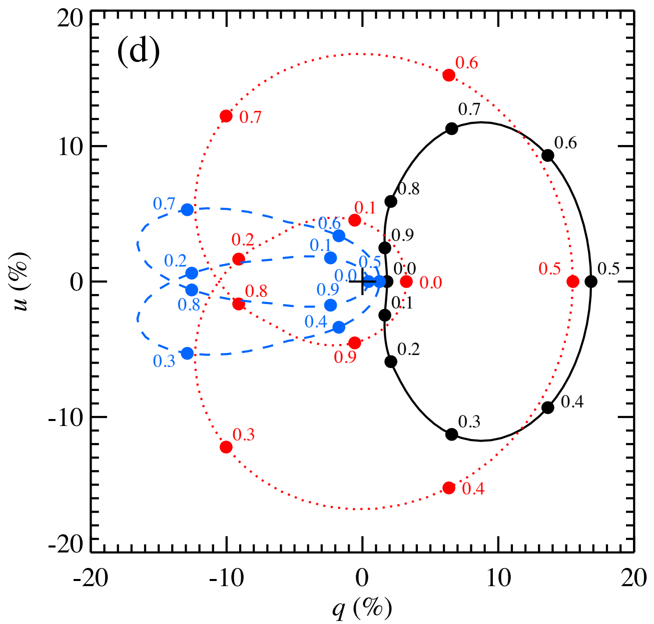

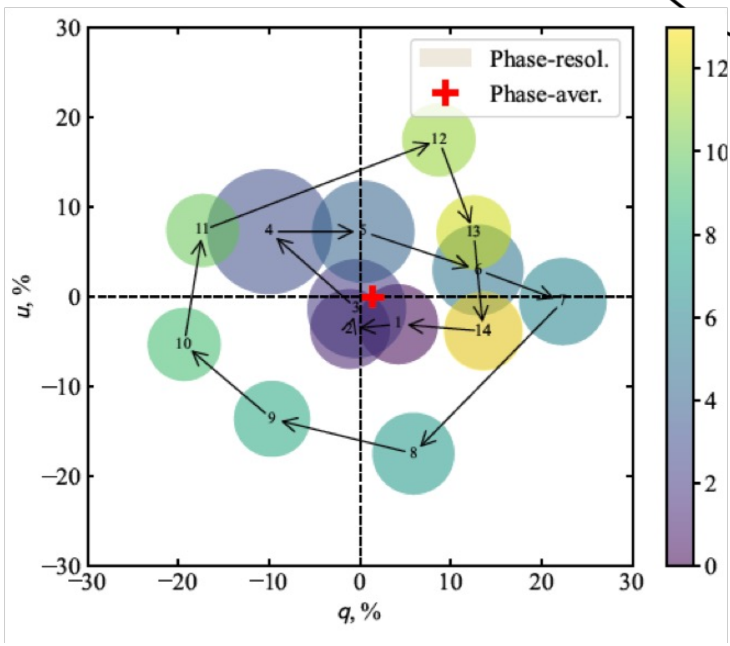

IXPE Imaging X-Ray Polarimetry Explorer

Photon propagation in the magnetosphere

▪ QED effects – Rotating Vector Model

- Strong magnetic fields polarize the virtual e^--e^+ pairs around the star

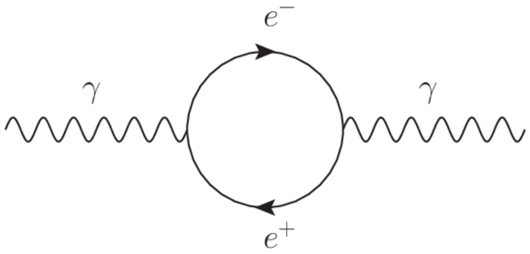

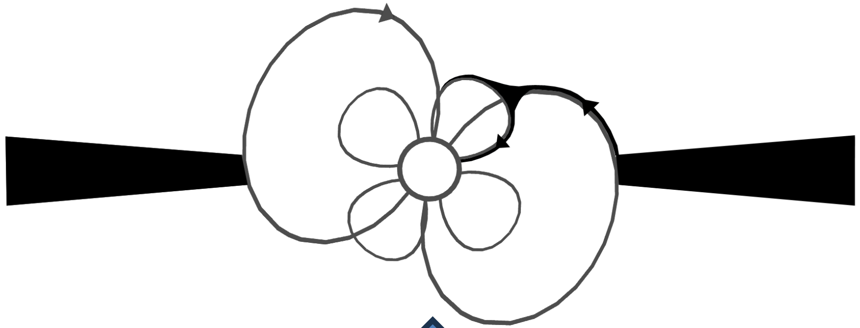

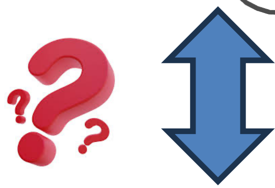

- The photon E-field is forced to adiabatically follow the star magnetic field along the photon trajectory

- Photon polarization vectors decouple from the B-field at large distances (adiabatic radius; where the magnetic field is ≈ a dipole)

Poutanen 2020

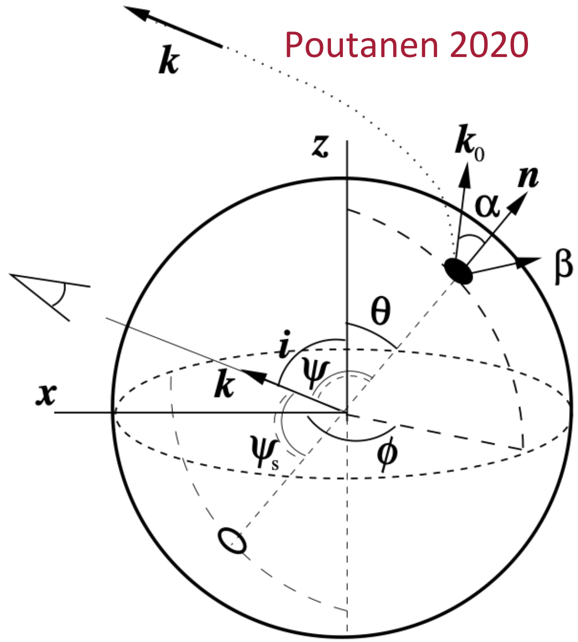

Photon propagation in the magnetosphere

- **QED vacuum polarization effects**
  - The limit within which polarization modes are preserved depends on the star magnetic field strength and photon energy

$$\frac{r_{\rm pl}}{R_{\rm NS}} \simeq 4.8 \left(\frac{\hbar\omega}{1\ \rm keV}\right)^{1/5} \left(\frac{B_{\rm p}}{10^{11}\ \rm G}\right)^{2/5} \left(\frac{R_{\rm NS}}{10\ \rm km}\right)^{1/5}$$

– PD is still determined by surface emission properties
– PA is independent of the B-field topology at the surface but reflects the magnetic dipole geometry. We expect PA to follow rotating vector model (RVM) (Radhakrishnan & Cooke 1969)

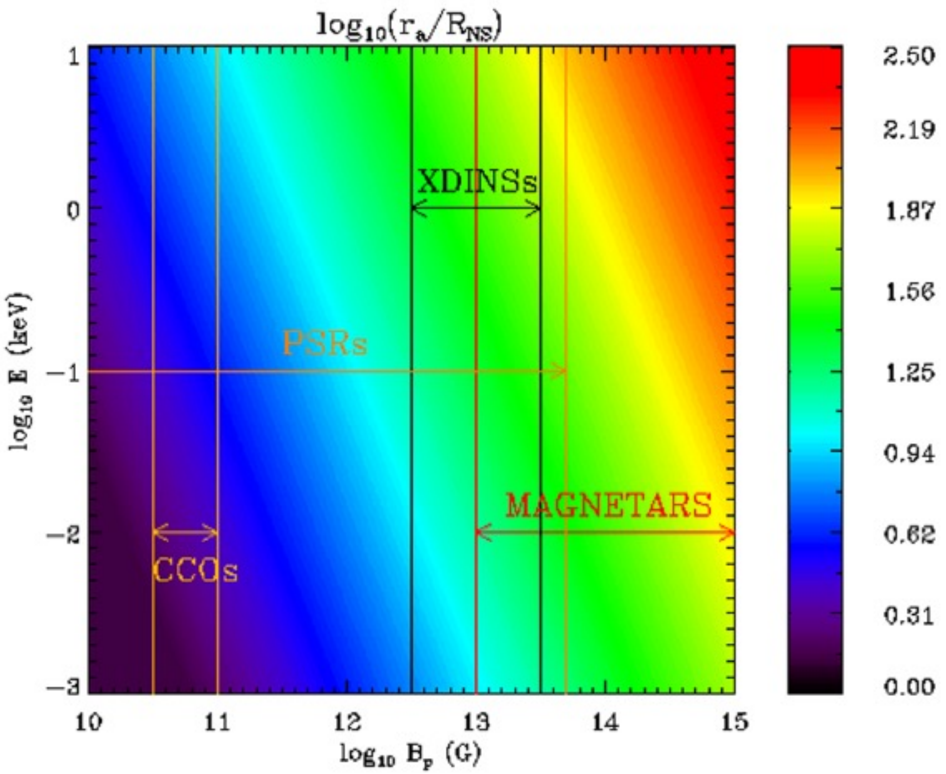

Taverna et al. (2015)

Rotating vector model -> geometry

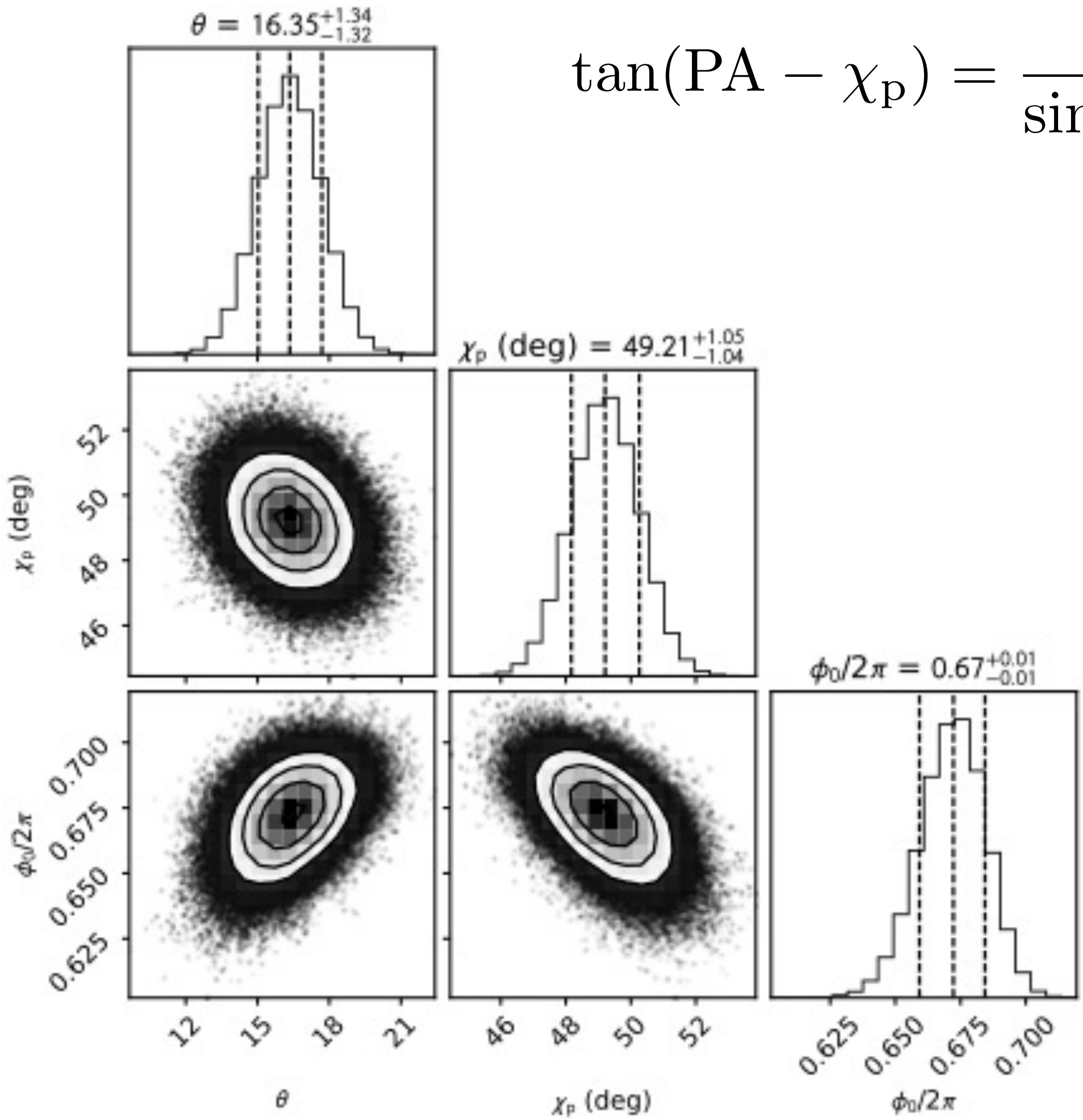

$$\tan(\mathrm{PA}-\chi_{\mathrm{p}}) = \frac{-\sin\theta\ \sin(\phi-\phi_0)}{\sin i_{\mathrm{p}}\cos\theta - \cos i_{\mathrm{p}}\sin\theta\cos(\phi-\phi_0)}$$

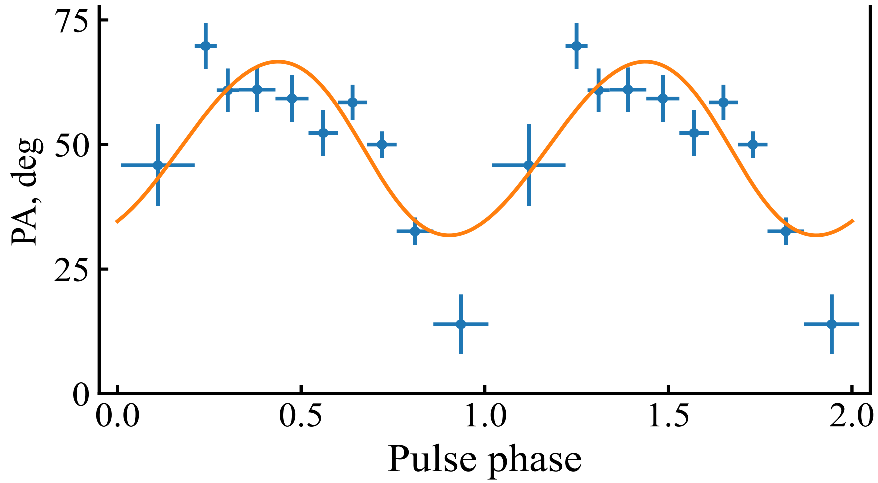

Tsygankov+, 2022, ApJL

IXPE observations of Her X-1

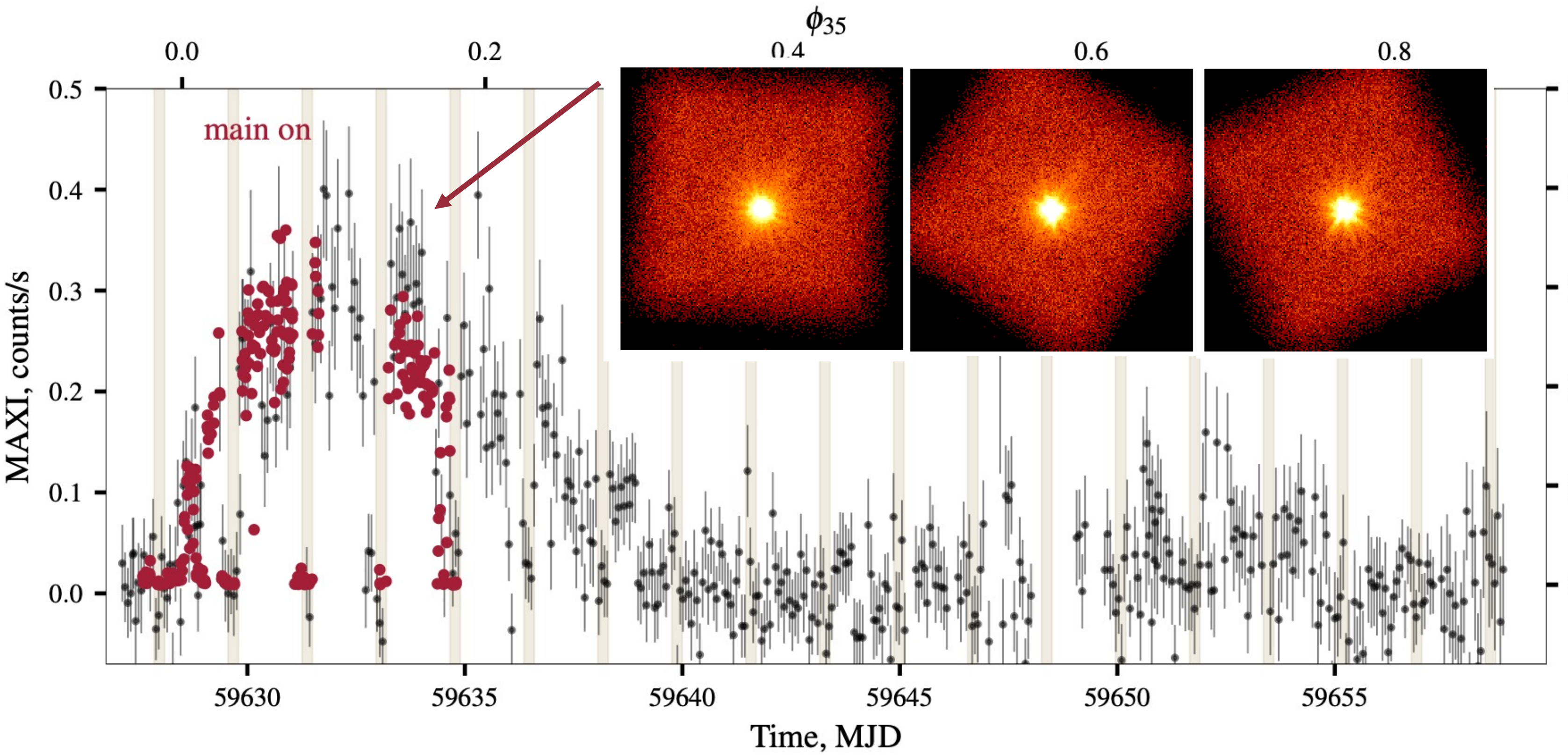

- Spin period: 1.24 s
- Orbital period: 1.7 d
- Super-orbital period: 35 d

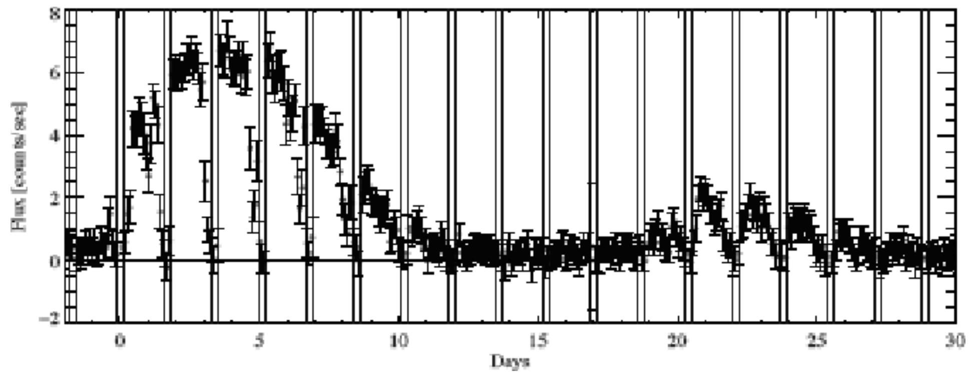

Doroshenko+, 2022, NatAst

Time dependence of X-ray polarization

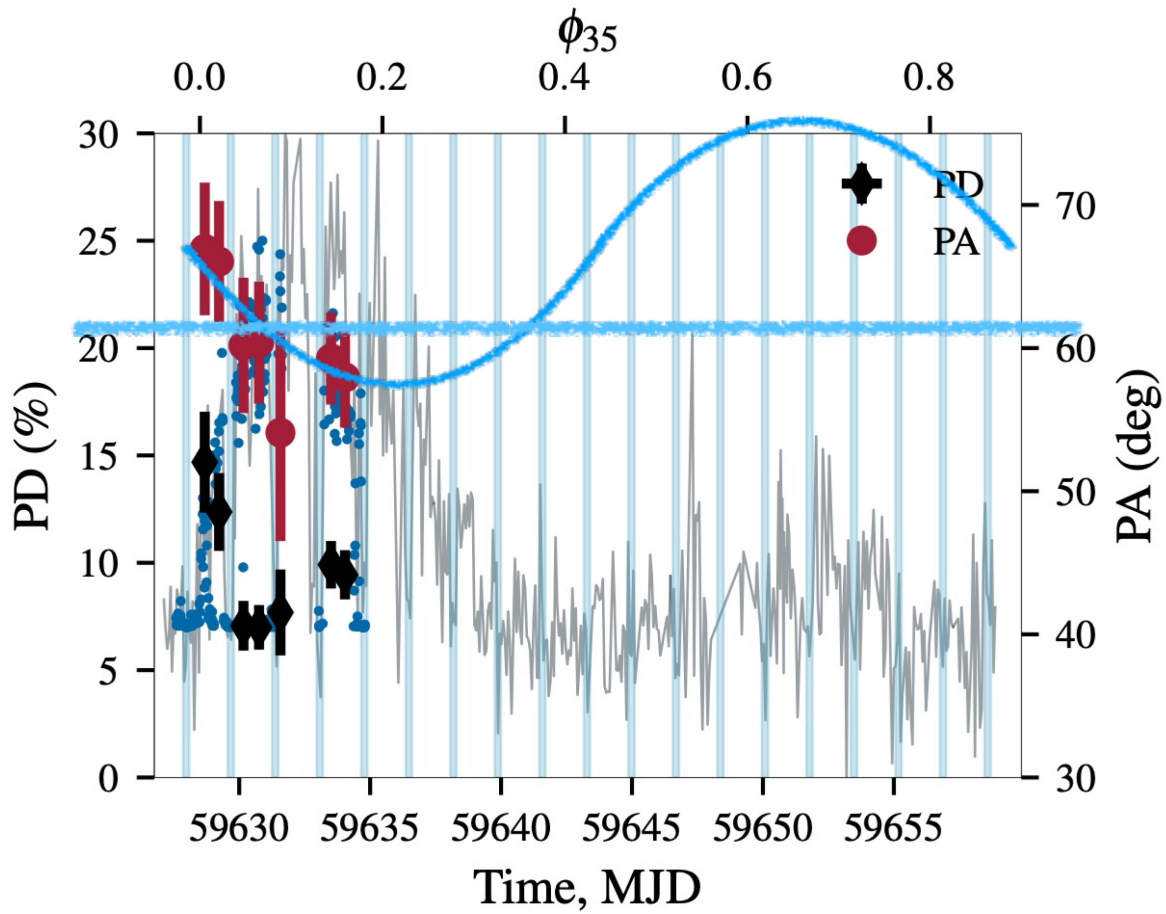

- Variability of both PD/PA with time (not very significant)
- More observations during the short-on are needed to check if average PA or amplitude of its variations change.

Second observation of Her X-1

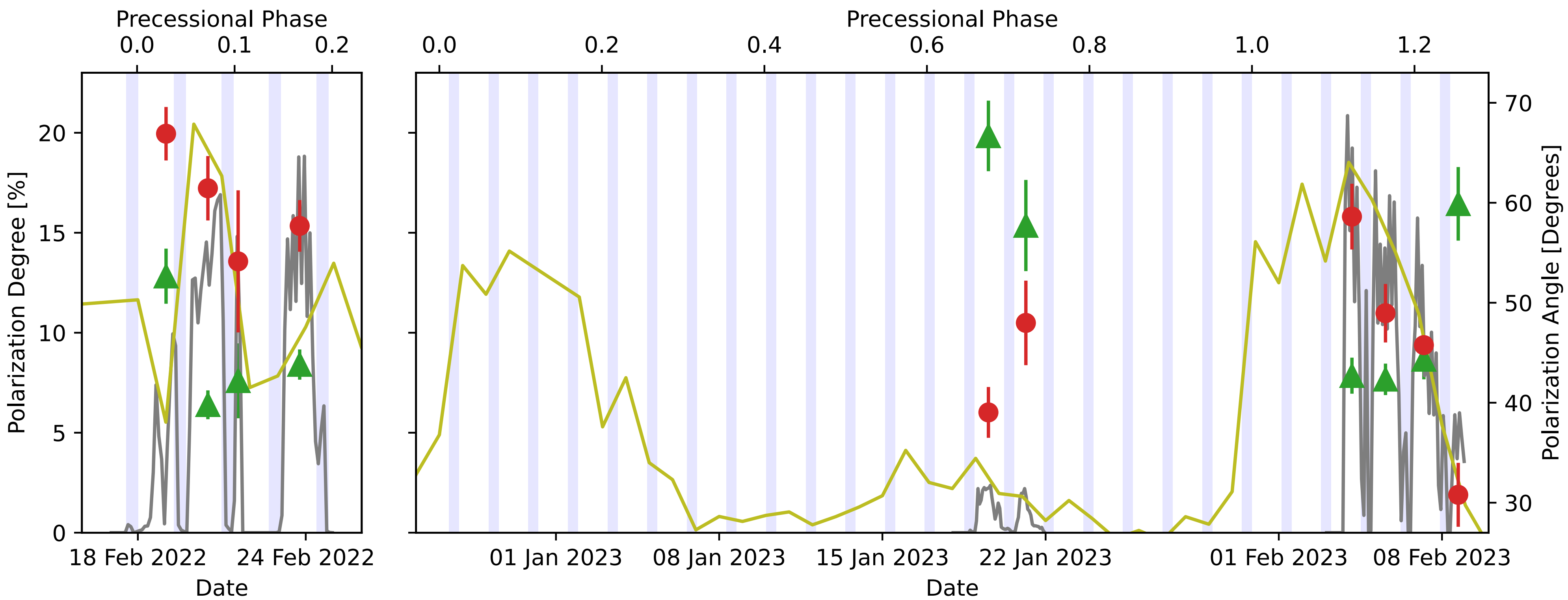

Heyl+, NatAst, 2024.

Second observation of Her X-1

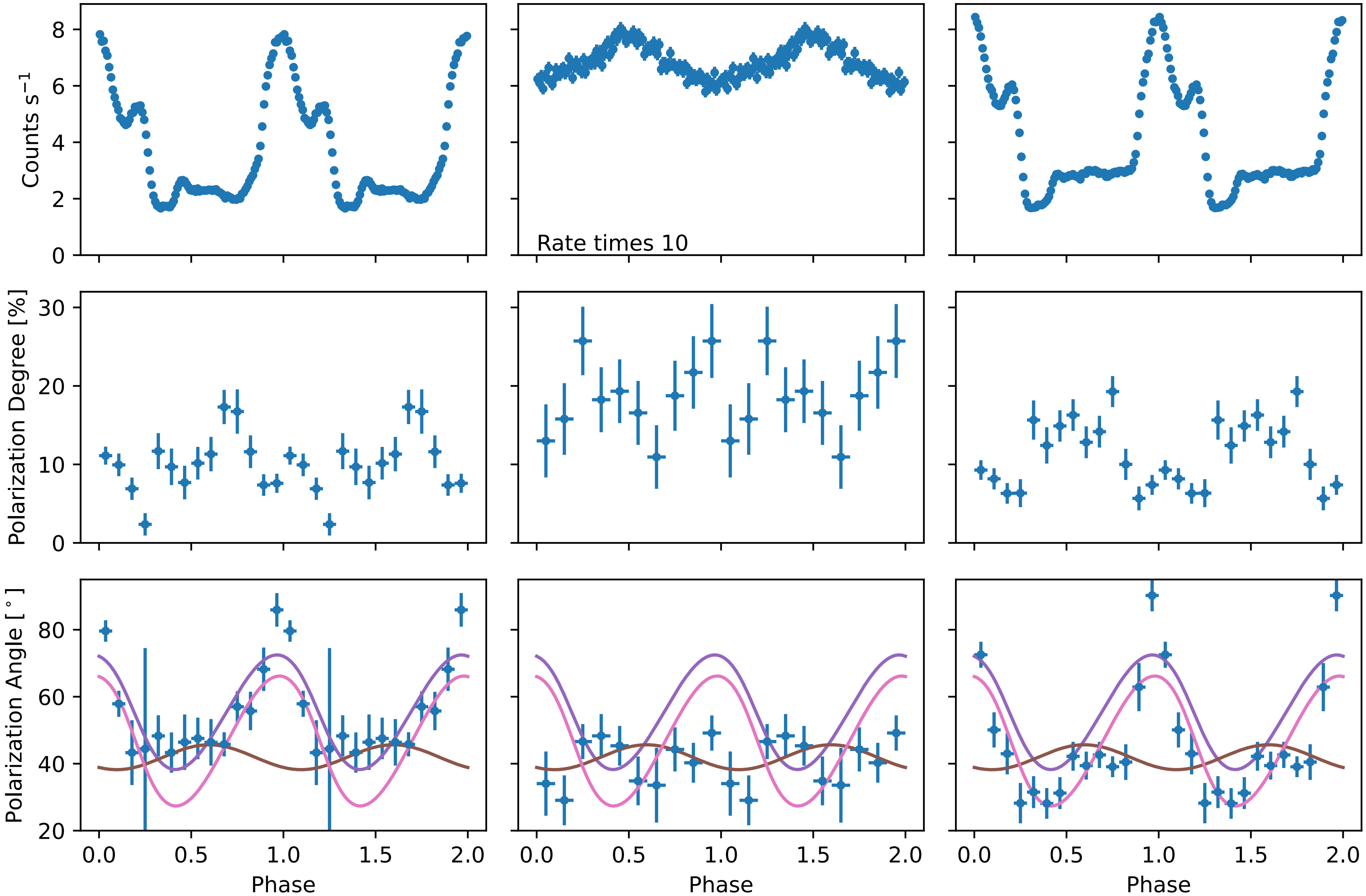

Heyl+, NatAst, 2024.

IXPE
Imaging X-Ray Polarimetry Explorer

Second observation of Her X-1

	Mean PD (%)	i_p (deg)	θ (deg)	χ_p (deg)	ϕ_0 (%)	Prec. Phase (%)
First Main-On	9.5 ± 0.5	58^{+28}_{-22}	$14.5^{+3.0}_{-4.0}$	55.4 ± 1.6	$19.0^{+2.7}_{-2.2}$	8.8
Early	8.6 ± 0.6	64^{+25}_{-22}	$16.3^{+3.5}_{-4.1}$	57.9 ± 2.1	$19.0^{+2.6}_{-2.4}$	7.3
Late	9.3 ± 0.7	85^{+35}_{-37}	$15.9^{+3.6}_{-4.0}$	52.2 ± 2.7	$21.7^{+4.5}_{-5.0}$	16.2
Short-On	17.8 ± 1.4	90^{+30}_{-30}	$3.7^{+2.6}_{-1.9}$	41.9 ± 2.2	85.1^{+18}_{-19}	68.7
Second Main-On	9.1 ± 0.5	56^{+24}_{-20}	$16.0^{+3.1}_{-4.3}$	46.8 ± 1.5	$19.8^{+2.3}_{-2.0}$	15.9

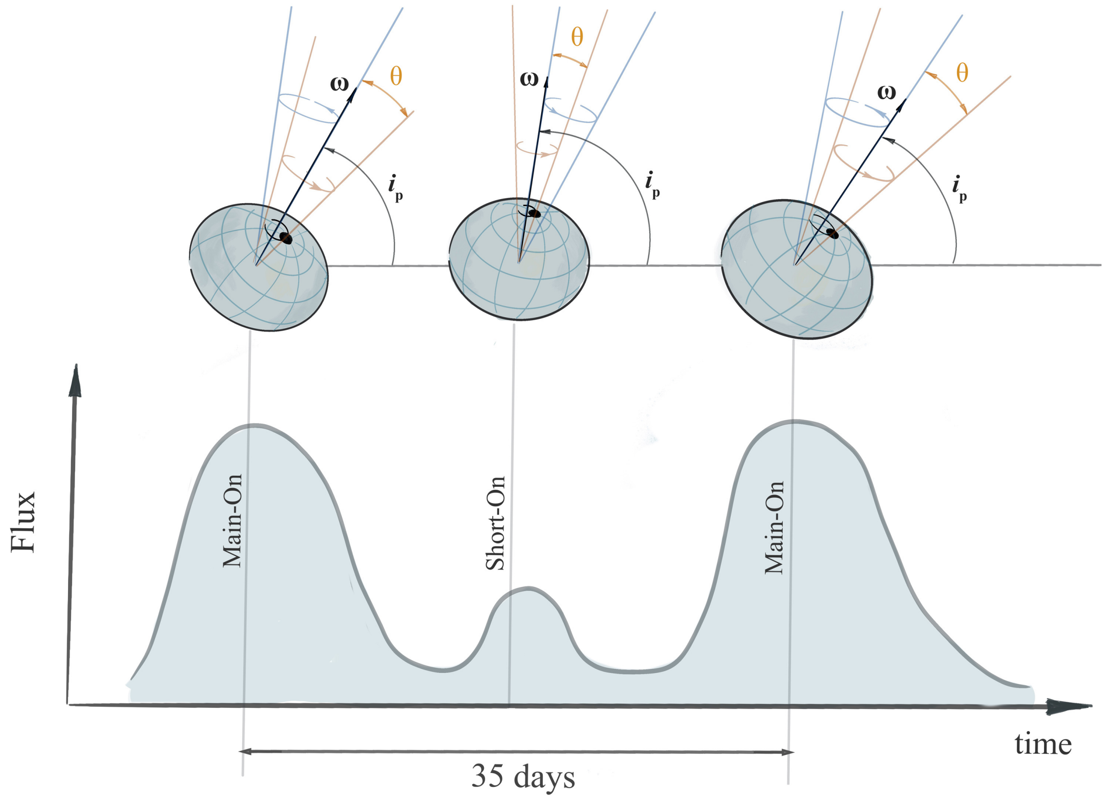

Heyl+, NatAst, 2024.

IXPE observations of Vela X-1

Persistent X-ray pulsar accreting from a wind. Pulsations with period P_s=283 s was discovered in 1975 by Rappaport & McClintock et al. using SAS-3.

Eclipses every 9 days by OSO-7 (Ulmer et al. 1972). Orbital period P_{orb}=8.964 d. Eclipse of 1.7 d duration.

Distance d=2 kpc.

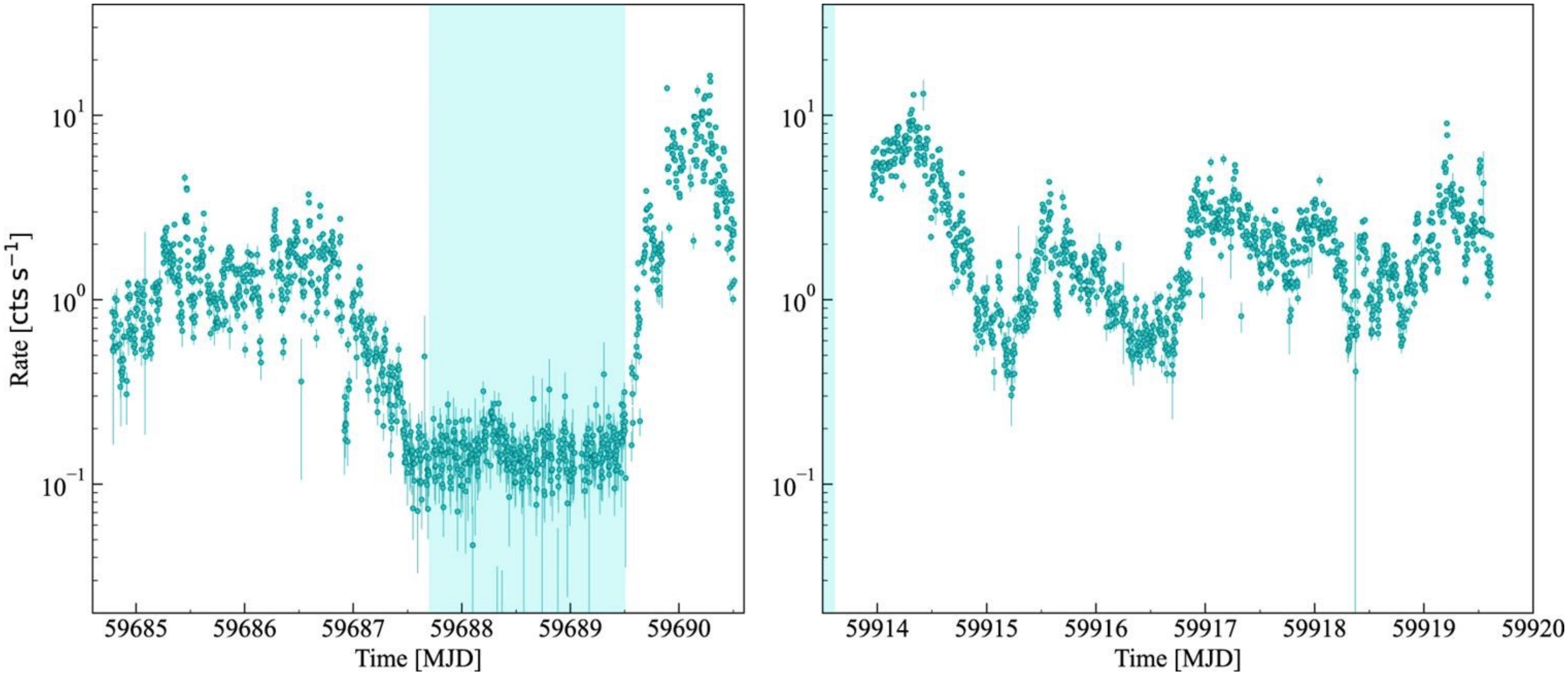

Forsblom+, 2023, ApJL

IXPE observations of Vela X-1

- Clear energy-dependence of polarization properties in the phase-averaged polarimetric analysis:
    1. The energy-resolved analysis shows the PD above 5 keV reaching 6%–10%

    2. ~90° swing in the PA between low and high energies

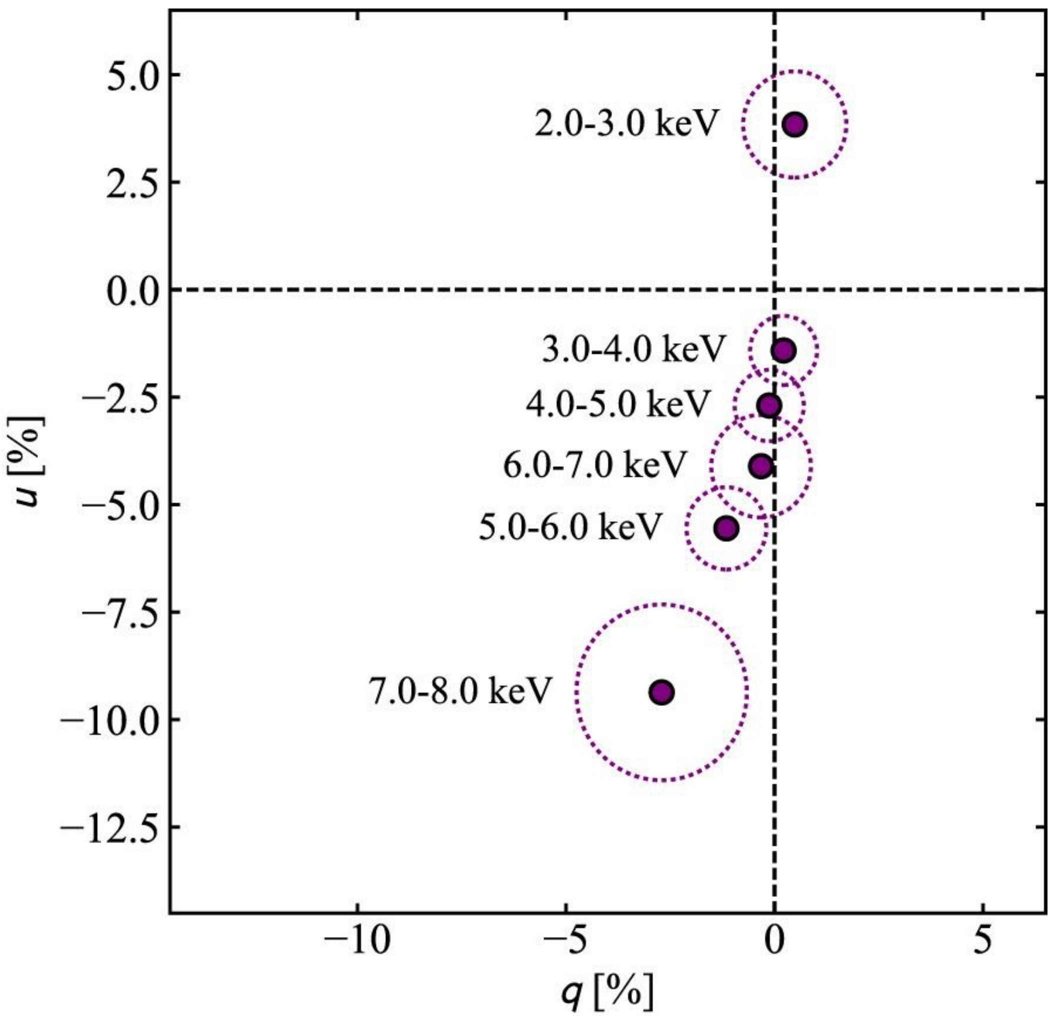

Forsblom+, 2023, ApJL

IXPE observations of LS V +44 17/RX J0440.9+4431

Active for the first time since 2010-11, onset of a Giant (Type II) outburst in Jan 2023

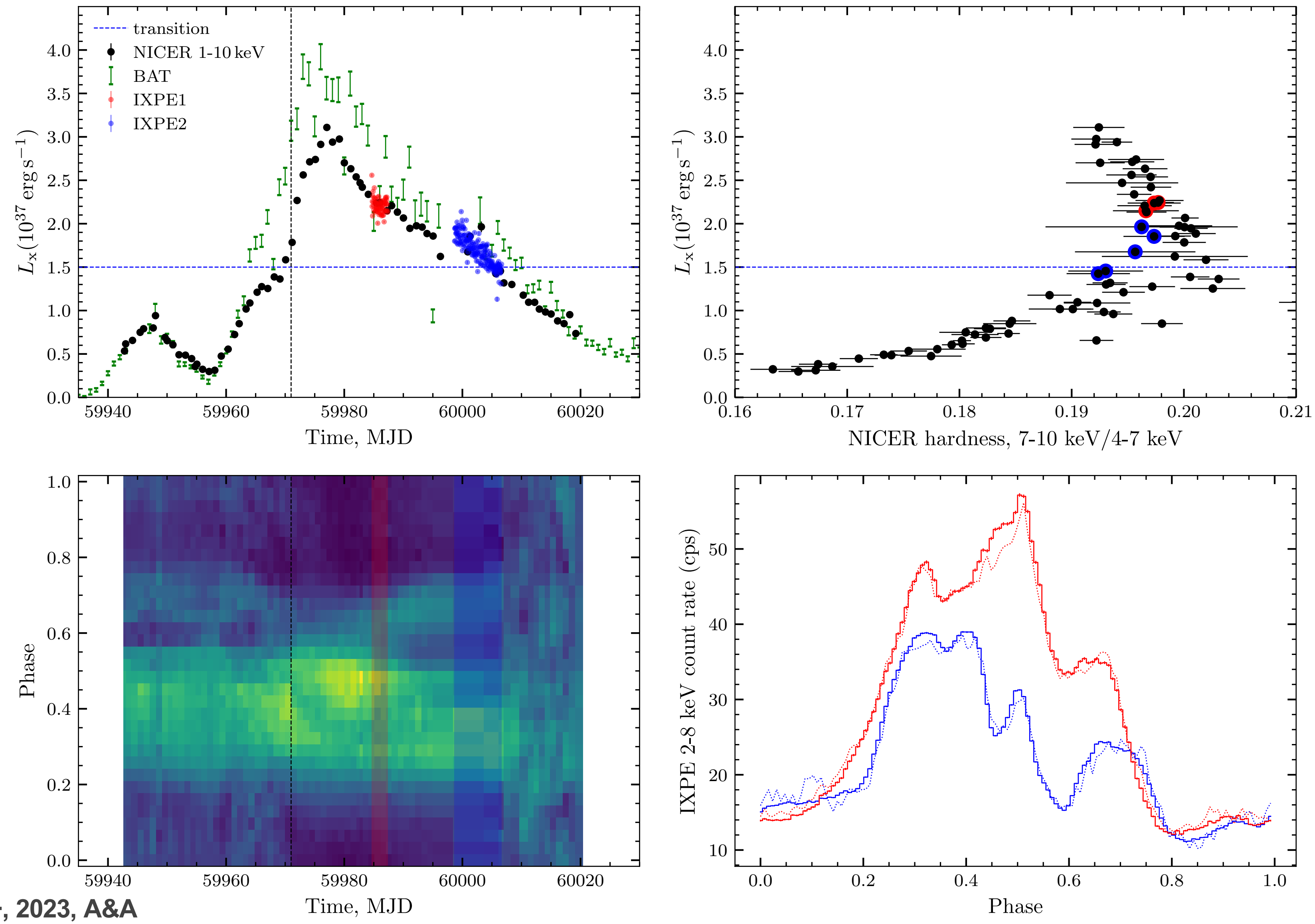

Doroshenko+, 2023, A&A

IXPE observations of LS V +44 17/RX J0440.9+4431

IXPE Imaging X-Ray Polarimetry Explorer

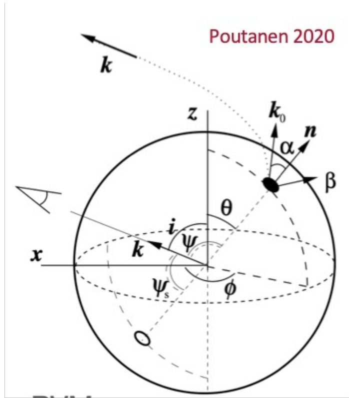

RVM:

$$\tan(\chi-\chi_{\rm p})=\frac{-\sin\theta\,\sin[2\pi(\phi-\phi_0)]}{\sin i_{\rm p}\cos\theta-\cos i_{\rm p}\sin\theta\cos[2\pi(\phi-\phi_0)]}$$

Exquisite statistics, yet like other XRPs both observations consistent with the Rotating Vector model (RVM, Radhakrishnan&Cooke 1969)

PCUBEs results consistent with simplified (power-law/CompTT) spectro-polarimetry

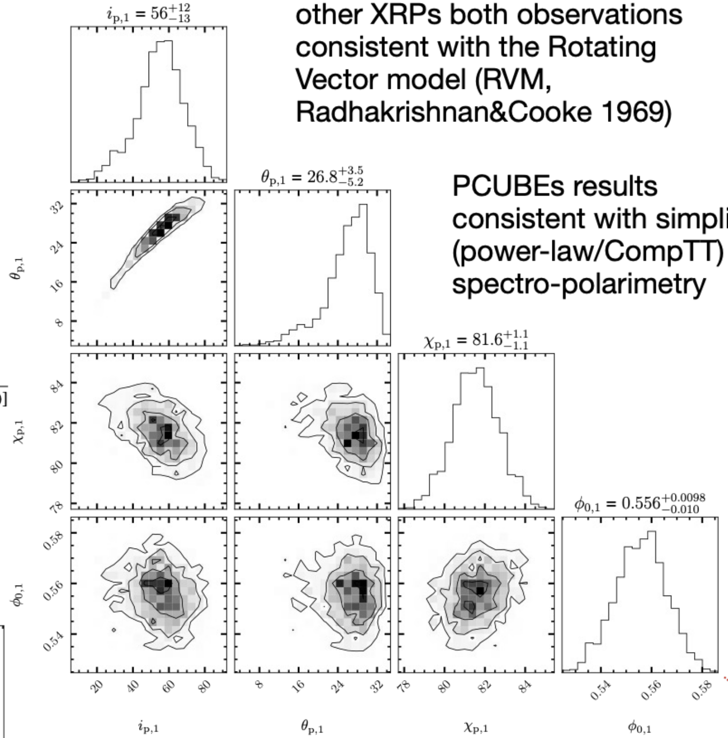

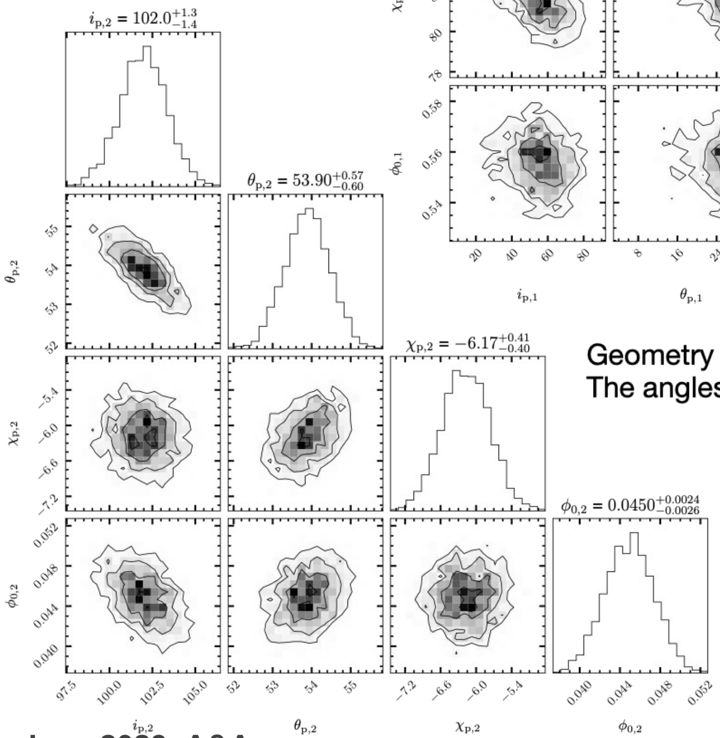

Geometry is dramatically different. The angles changed by

$\Delta i_p \sim 46^\circ$

$\Delta \theta_p \sim 30^\circ$

$\Delta \chi_p \sim 90^\circ$

$\Delta \phi_0 \sim 0.5$

…in 10 days

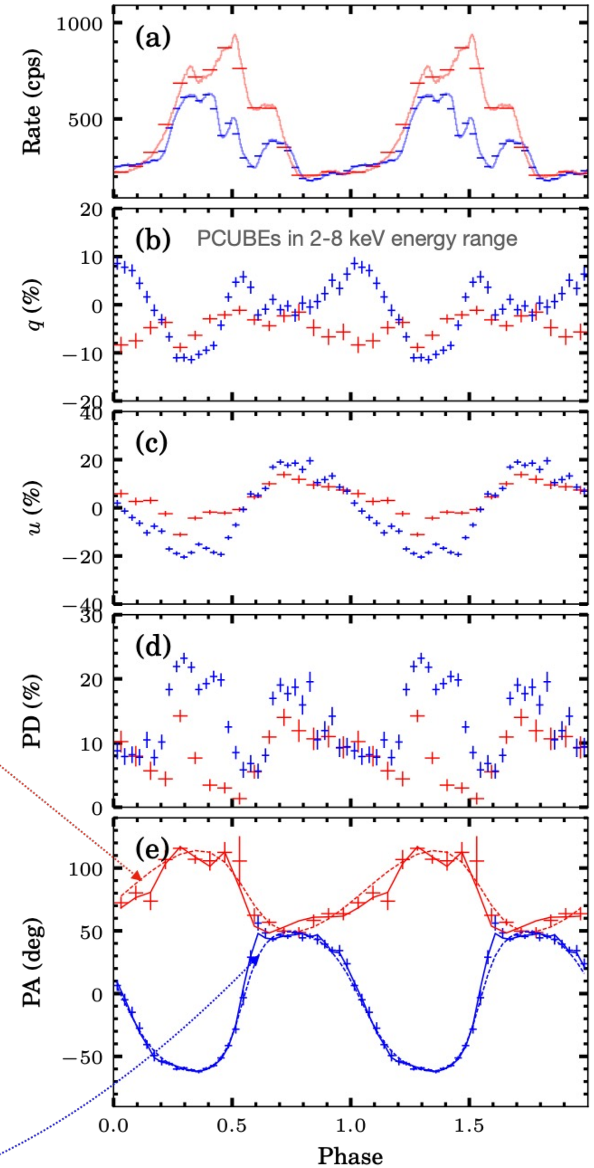

Doroshenko+, 2023, A&A

IXPE observations of LS V +44 17/RX J0440.9+4431

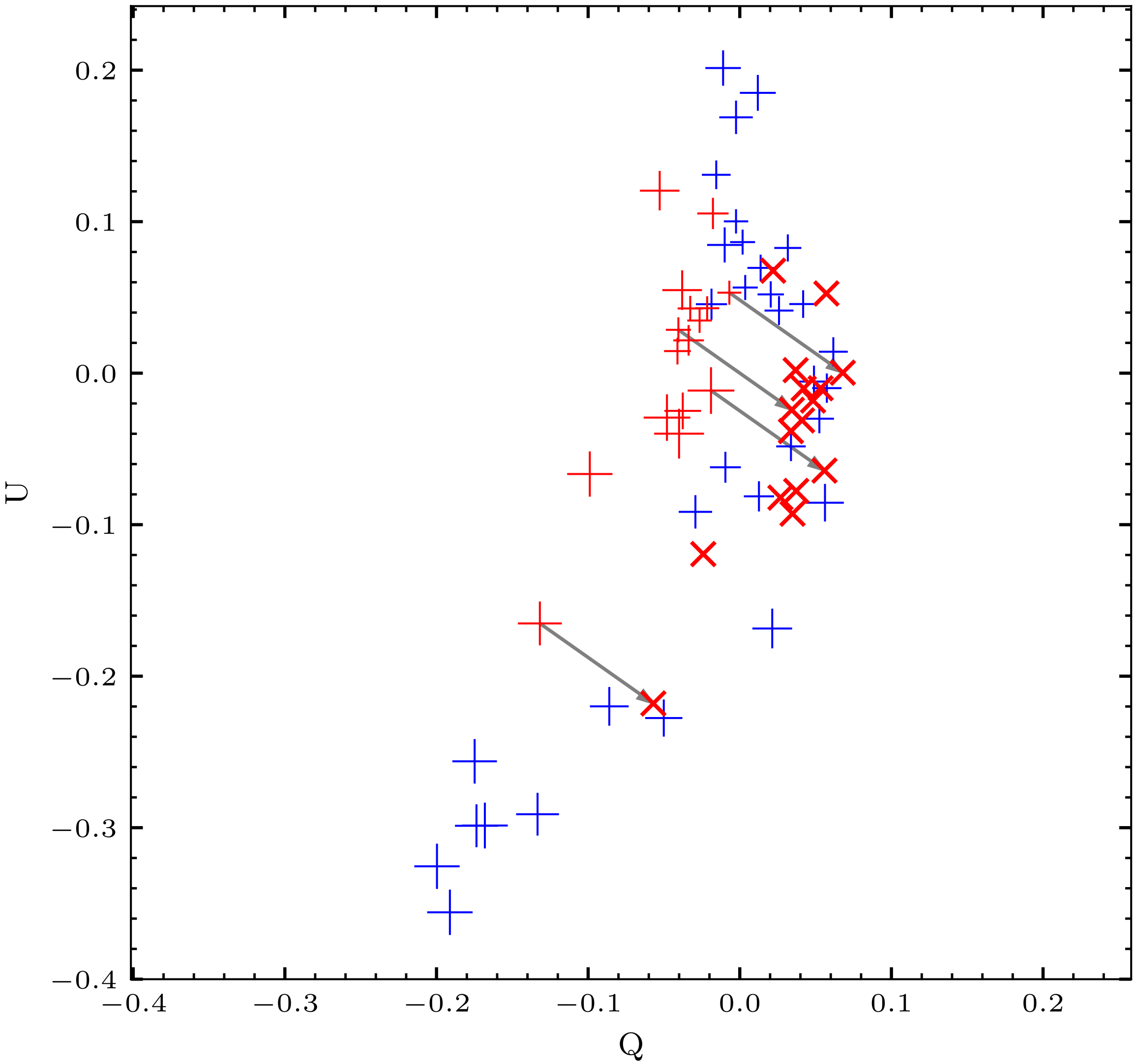

There appears to be a constant shift in Q/U space between the two observations, i.e. additional constant polarised component? Re-define the model…

IXPE observations of LS V +44 17/RX J0440.9+4431

Work in Q/U space

$$
\begin{aligned}
I(\phi) &= I_0 + I_1(\phi),\\
Q(\phi) &= Q_0 + P_1(\phi) I_1(\phi) \cos[2\chi(\phi)],\\
U(\phi) &= U_0 + P_1(\phi) I_1(\phi) \sin[2\chi(\phi)].
\end{aligned}
$$

observed constant RVM-part

$$
\tan(\chi - \chi_{\rm p}) = \frac{-\sin\theta \, \sin[2\pi(\phi-\phi_0)]}{\sin i_{\rm p}\cos\theta - \cos i_{\rm p}\sin\theta\cos[2\pi(\phi-\phi_0)]}
$$

- Assume constant + RVM components
- RVM parameters constrained through comparison with observed Q/U
- **Only $I_{0,1}$x$P_{0,1}$ is constrained, not flux P individually** *(can have low-intensity strongly polarised background or high-intensity weakly polarised background)*
- Some limits can be obtained based on conditions $I_0<I_{1,min}$, $P_0<1$, $P_1<1$, $P_0>P_0(I_0/I_{min})$

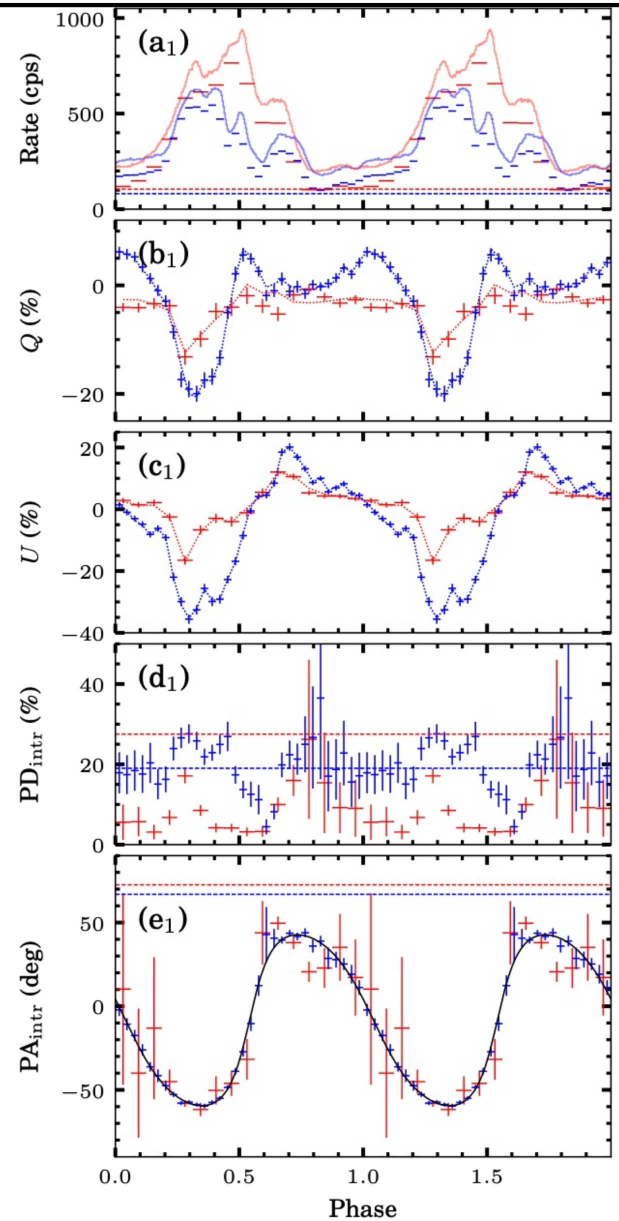

(after subtracting constant component)

Doroshenko+, 2023, A&A

IXPE observations of LS V +44 17/RX J0440.9+4431

•Three questions:
- what is it?
- can it give 10-40% of observed flux?
- 30% polarisation?

•Unpulsed = relatively far away from NS: scattering in disk/disk wind?
- **PD up to ~33%** due to comptonization in accretion disk atmosphere (Sunyaev&Titarchuk 1985) or outflows
  - **~20% polarization** observed in Cyg X-3/Circinus (scattering)
- There's evidence for presence of strong disk outflows in BeXRBs from radio and X-ray data (Jaisawal et al. 2019; Doroshenko et al 2020, van den Eijnden et al. 2019, 2022; Chatzis et al. 2022; van den Eijnden et al. 2022) with **up to 20% flux in reflected/scattered component** (although at higher L_x).
- LS V +4417 is viewed **~edge-on**, polarization due to scattering is expected to be high (i.e. fraction of scattered emission may remain low)

Geometries of different XRPs

Her X-1

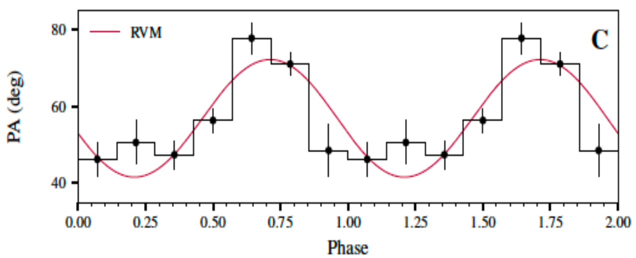

Cen X-3

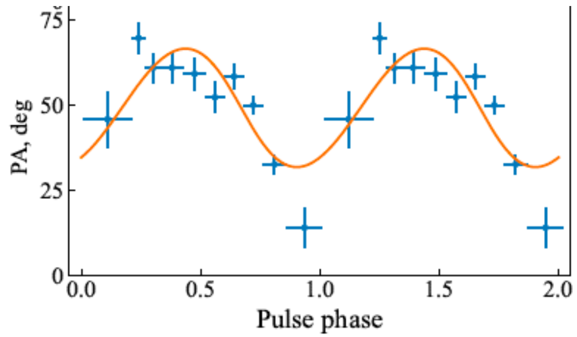

X Persei

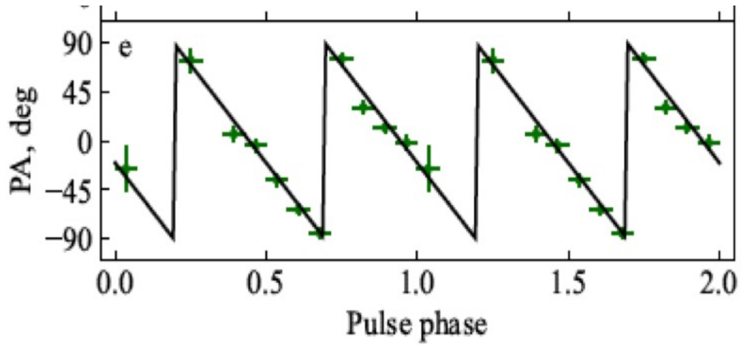

GX 301-2

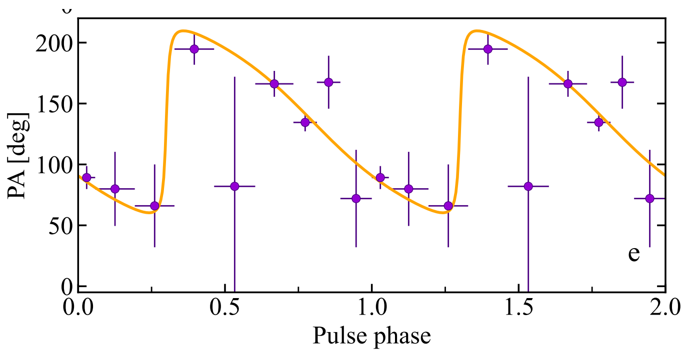

GRO J1008-57

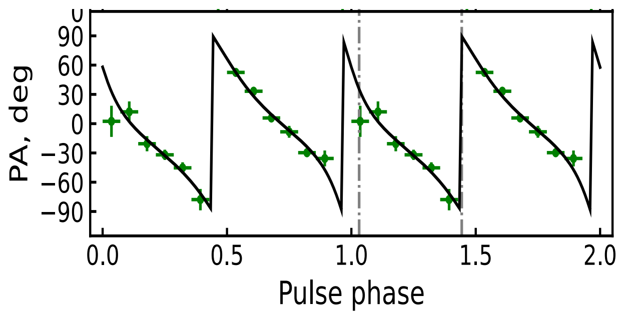

EXO 2030+375

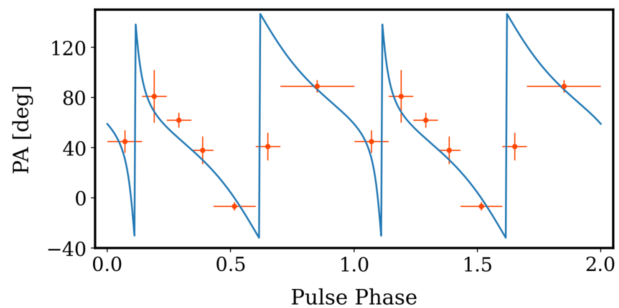

IXPE
Imaging
X-Ray
Polarimetry
Explorer

Marshall Space Flight Center
agenzia spaziale italiana

Geometries of different XRPs

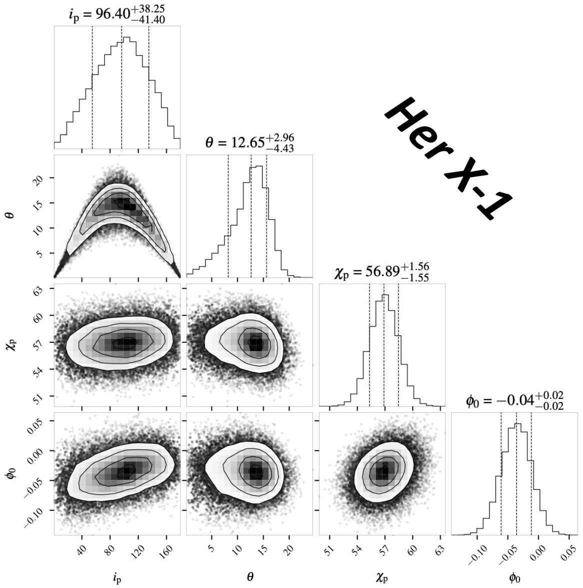

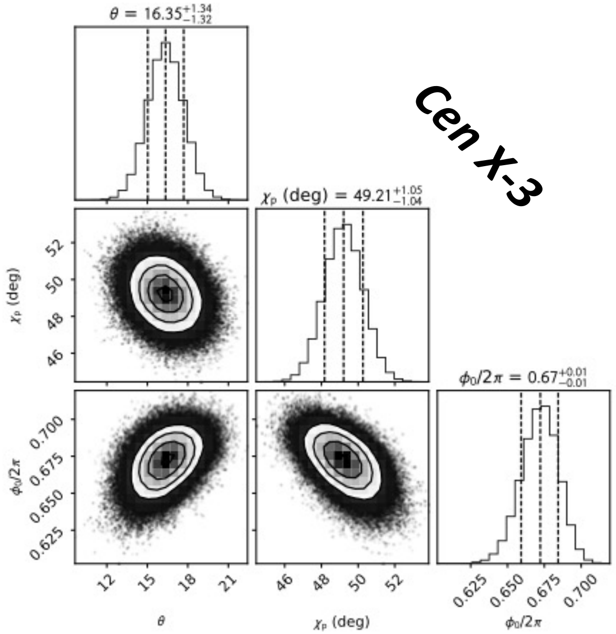

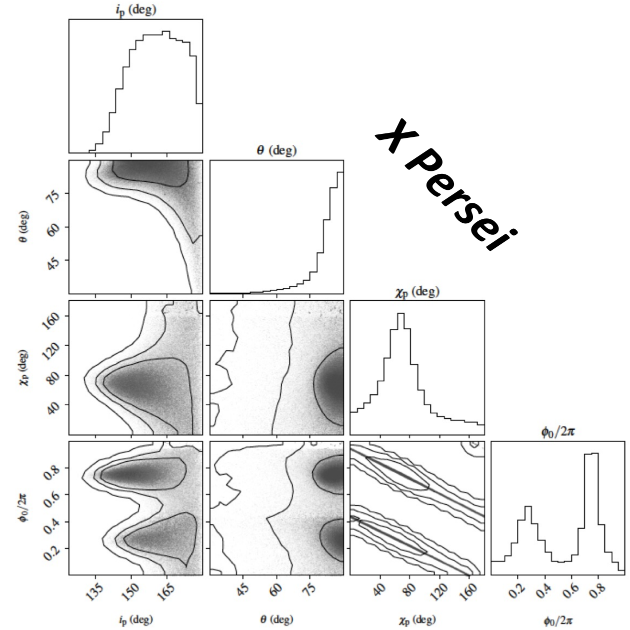

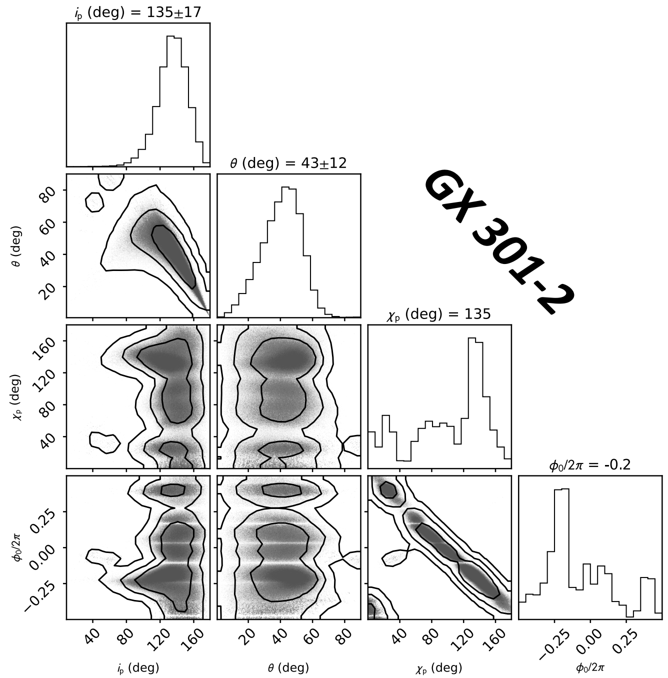

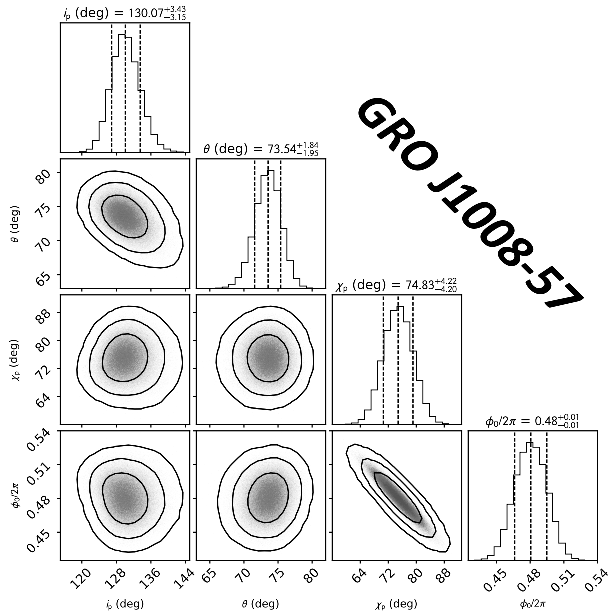

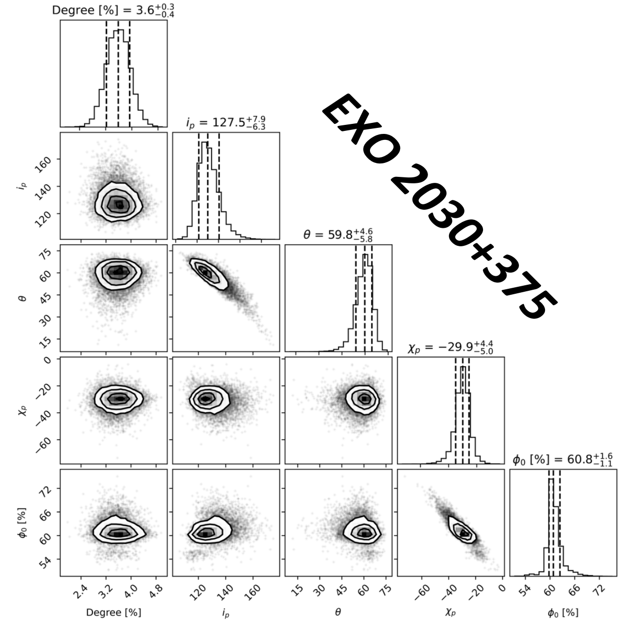

Low polarization degree

IXPE
Imaging
X-Ray
Polarimetry
Explorer

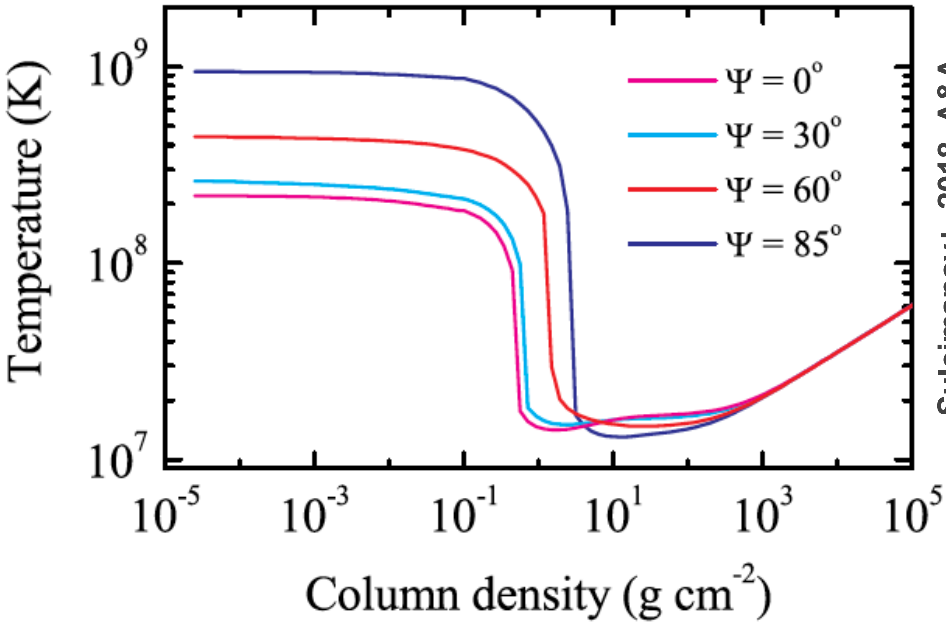

Suleimanov+, 2018, A&A

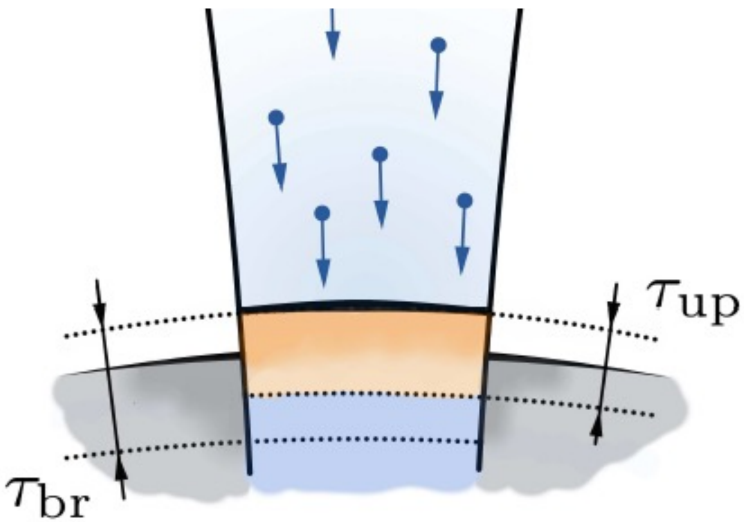

Mushtukov+, 2021,MNRAS, 503

What happens at low luminosity state?

- Sub-critical regime of accretion.
- Plasma braking in the atmosphere of a NS.
- Overheated upper layer.
- Resonant scattering above NS surface.

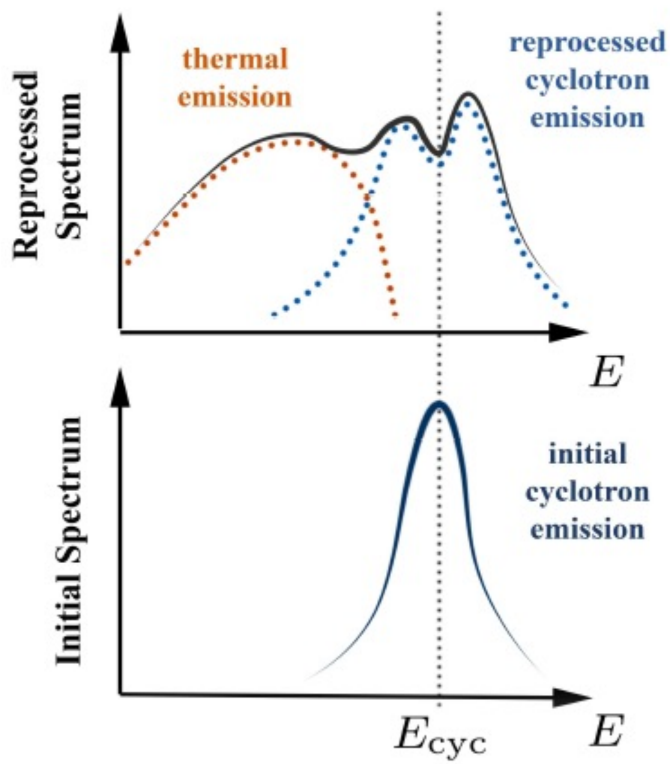

IXPE
Imaging
X-Ray
Polarimetry
Explorer

Low polarization degree

- **Normally T decreases going outwards**
- **X-mode photon photosphere is deeper than the O-mode ⇒**
  X-mode dominates flux
- **Particle bombardment produces inverted T gradient, O-mode photons escape at a larger temperature, and may dominate the outgoing flux**
- **Polarization depends on the thickness of the heated layer.**

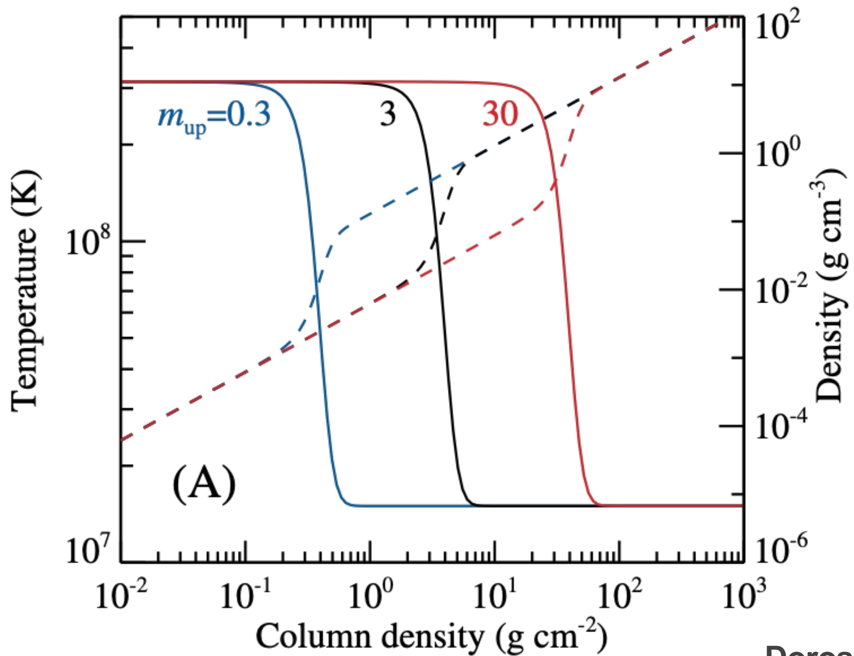

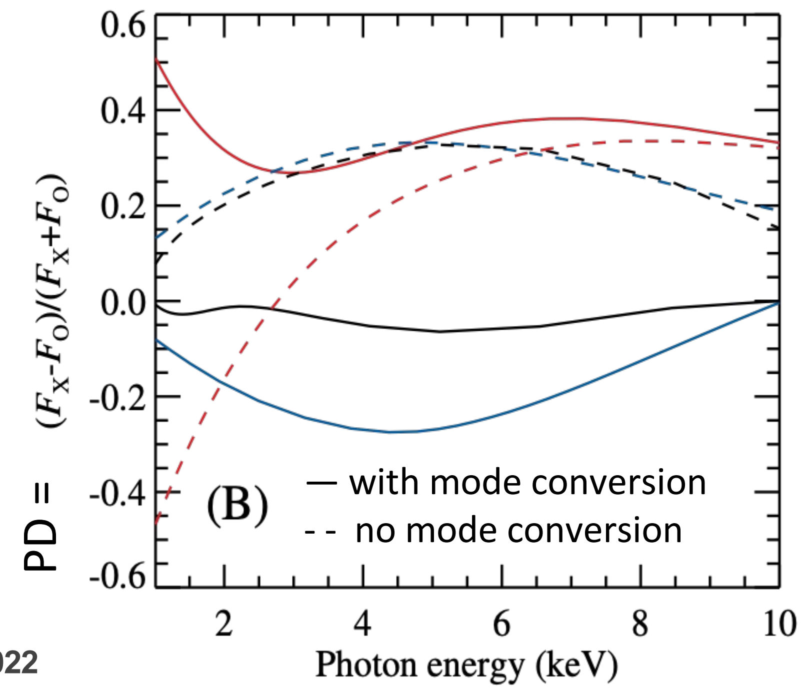

Doroshenko+, 2022

Conclusions

IXPE has opened a new window to the Universe. Observations of X-ray polarization are already revolutionizing our understanding of highly magnetized neutron stars. In the first two years of the observatory's operation, we:

• Demonstrated that the degree of polarization is lower than expected even in bright pulsars.
• For the majority of XRPs, we measured the geometry; for all of them, the inclinations of the orbit and the pulsar are in agreement; magnetic inclinations have a wide distribution.
• Discovered a non-pulsating polarized emission component in a pair of bright pulsars.
• Detected that in Vela X-1, the polarization angle changes by 90 degrees at energies around 3 keV.
• Observed both correlation and anticorrelation of flux in the profile and degree of polarization.
• Confirmed the precession of the neutron star in Her X-1.

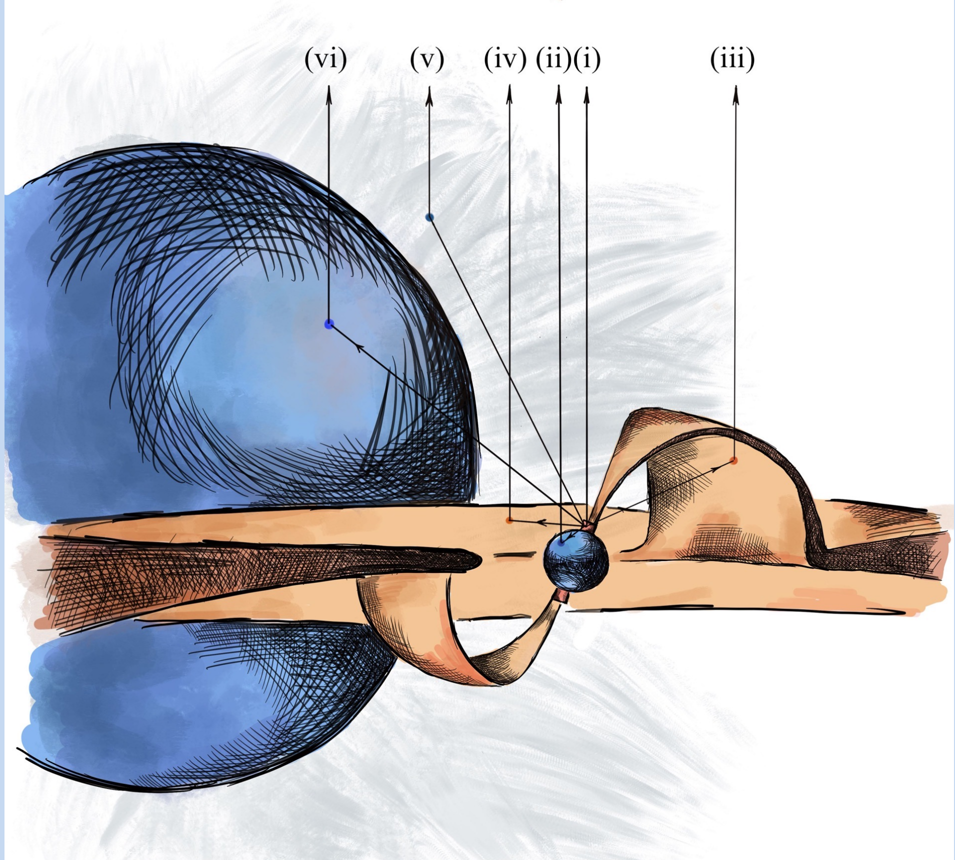

IXPE
Imaging X-Ray Polarimetry Explorer

Non-magnetized NSs

Circinus X-1

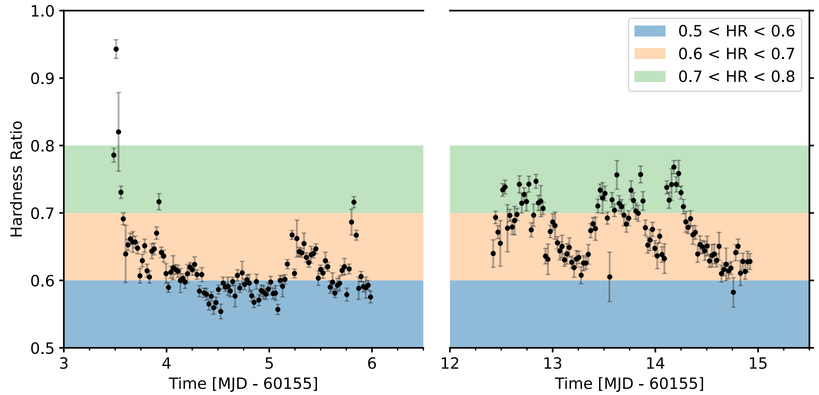

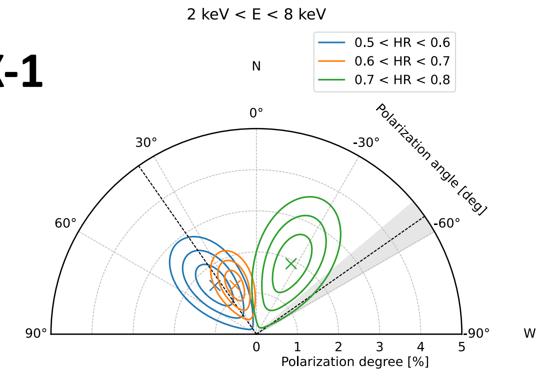

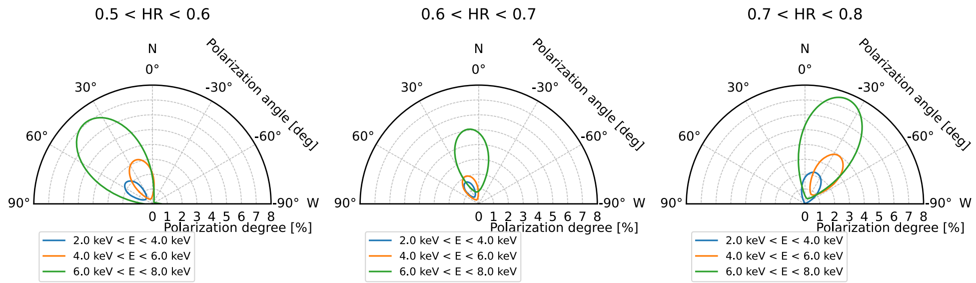

Rankin+, 2024

GX 13+1

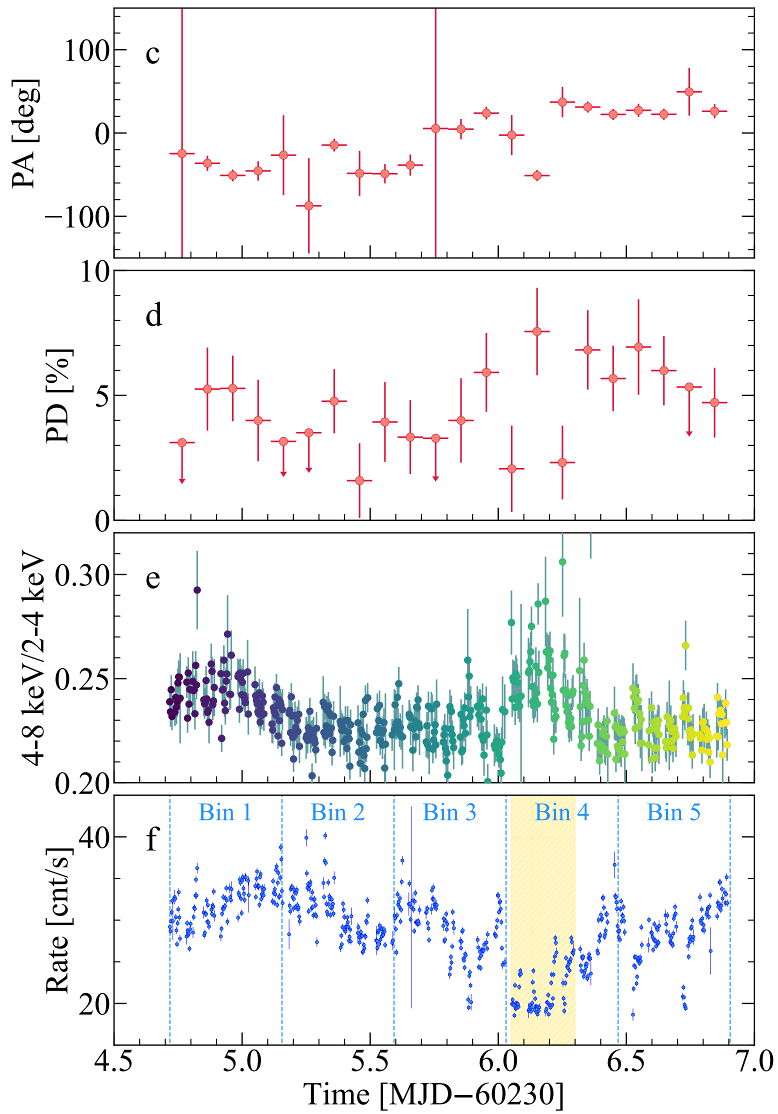

Bobrikova+, 2024

Imaging X-Ray Polarimetry Explorer

Non-magnetized NSs

Circinus X-1

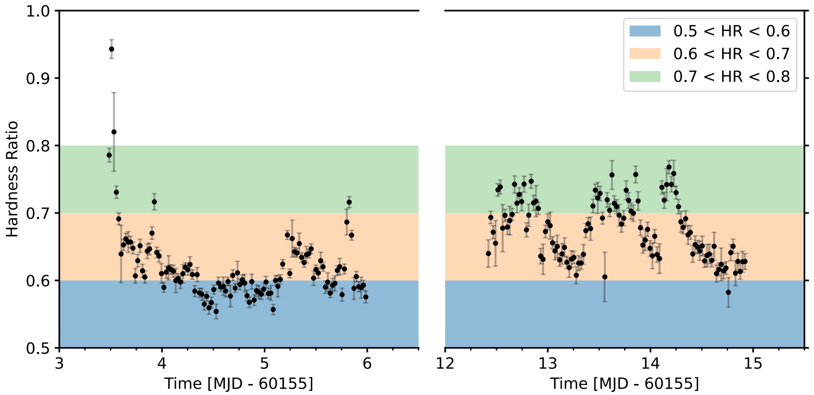

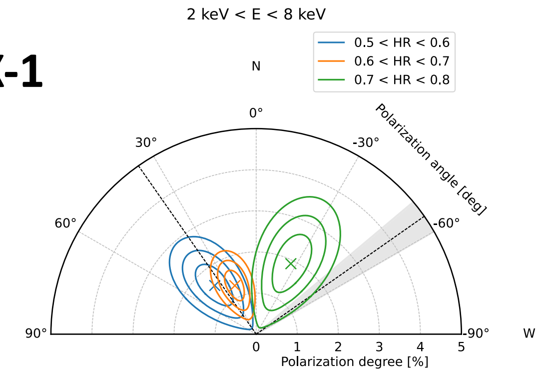

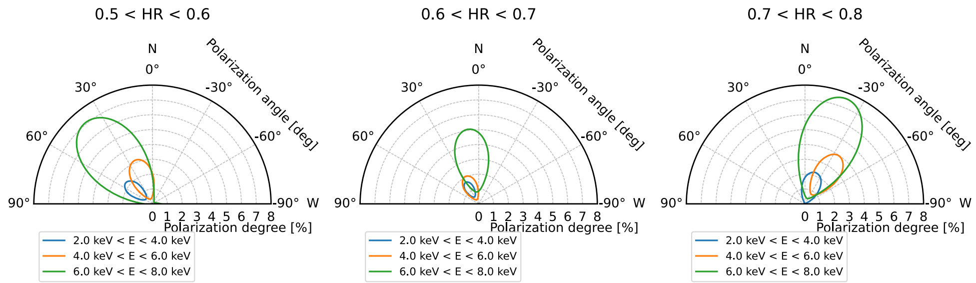

Rankin+, 2024

GX 13+1

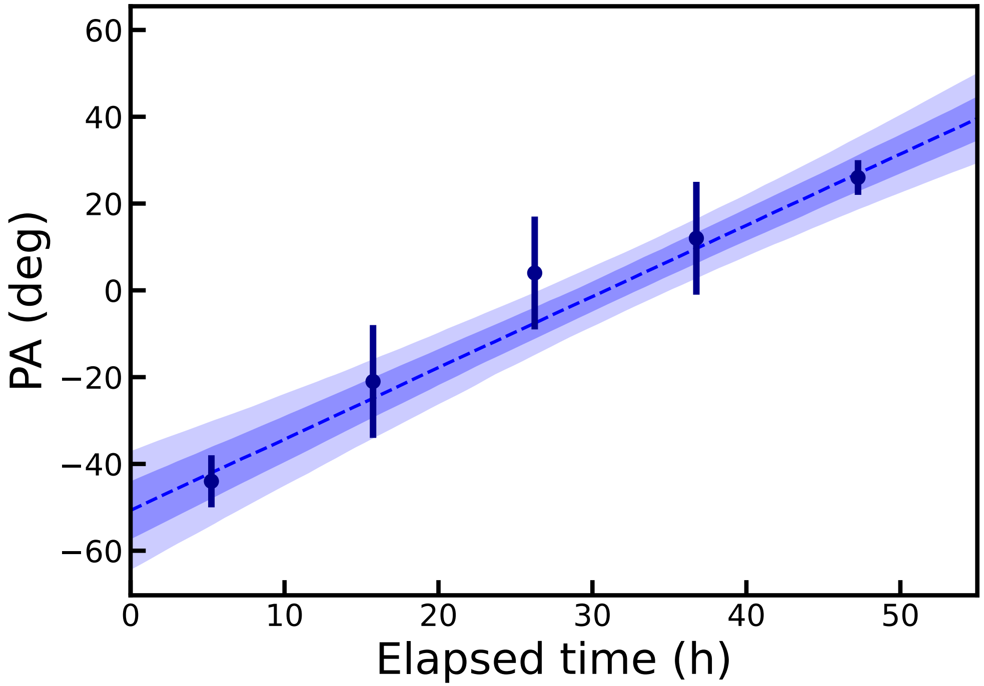

Bobrikova+, 2024

Non-magnetized NSs

Possible interpretation: the presence of a constant component of polarization, strong wind scattering, or different polarization of the two main spectral components with individually peculiar behavior. The rotation of the PA suggests a 30^{o}–40^{o} misalignment of the neutron star spin from the orbital axis.